İSTANBUL TECHNICAL UNIVERSITY ★ INSTITUTE OF SCIENCE AND TECHNOLOGY

DETECTING SHIP TRACKS and ESTIMATING THEIR MICROPHYSICAL PROPERTIES in the ATMOSPHERE WITH MODIS DATA

M. Sc. Thesis by
Burcu KABATAŞ

Department : Maritime Transportation Engineering

Programme : Maritime Transportation Engineering

JANUARY 2011

İSTANBUL TECHNICAL UNIVERSITY ★ INSTITUTE OF SCIENCE AND TECHNOLOGY

DETECTING SHIP TRACKS and ESTIMATING THEIR MICROPHYSICAL PROPERTIES in the ATMOSPHERE WITH MODIS DATA

M.Sc. Thesis by
Burcu KABATAŞ
(512081002)

Date of submission : **16 December 2010**
Date of defence examination: **26 January 2011**

Supervisor (Chairman) : **Assoc. Prof. Dr. Ata Bilgili (ITU)**
Co-Supervisor : **Prof. Dr. Paul Menzel (UW-Madison)**
Members of the Examining Committee : **Assoc. Prof. Dr. Alper Ünal (ITU)**
Assist. Prof. Dr. Münip Baş (ITU)
Assist. Prof. Dr. Serdar Kum (ITU)

JANUARY 2011

İSTANBUL TEKNİK ÜNİVERSİTESİ ★ FEN BİLİMLERİ ENSTİTÜSÜ

GEMİ İZLERİNİN SAPTANMASI ve ATMOSFERDEKİ GEMİ İZLERİNİN MİKROFİZİKSEL ÖZELLİKLERİNİN MODIS VERİSİ İLE HESAPLANMASI

YÜKSEK LİSANS TEZİ
Burcu KABATAŞ
(512081002)

Tezin Enstitüye Verildiği Tarih : 16 Aralık 2010
Tezin Savunulduğu Tarih : 26 Ocak 2011

Tez Danışmanı : Doç. Dr. Ata Bilgili (İTÜ)
Eş Danışman : Prof. Dr. Paul Menzel (UW-Madison)
Diğer Jüri Üyeleri : Doç. Dr. Alper Ünal (İTÜ)
Yard. Doç. Dr. Münip Baş (İTÜ)
Yard. Doç. Dr. Serdar Kum (İTÜ)

OCAK 2011

FOREWORD

I take this opportunity to express my heartfelt gratitude to my advisor Assoc. Prof. Ata BİLGİLİ for his help, guidance and patience in all stages of my work. I also would like to thank Prof. Paul MENZEL for being my co-adviser and giving me a chance to benefit from his experience while working with him at the University of Wisconsin- Madison. I am also grateful to Dr. Liam GUMLEY for inviting me to study at the University of Wisconsin Madison. He was an invaluable recourse and I greatly admire his patience and guidance.

I would like to express my gratitude to my family for supporting and trusting me at every step of my life. I am thankful for my beloved friends Utkan Kolat, Ruwan Ranatunga, Kaba Bah and Sajika Gallege for supporting me throughout my research and fiiling my life with joy. Furthermore, I would like to thank my trustworthy friends S. Saadet Kalender, M. Nezih Muşlu, Cihan Bulut and Cenk Avcı for their support and help.

Last but not least, I would like to thank all who have helped me and supported me throughout my research and my thesis.

December 2010

Burcu Kabataş

Maritime Transportation Engineer

TABLE OF CONTENTS

Page

ABBREVIATIONS

AATSR : Advanced Along-Track Scanning Radiometer
AMSR-E : Advanced Microwave Scanning Radiometer for EOS
ATBD : Algorithm Theoretical Basis Document
CCN : Cloud Condensation Nuclei
EOS-AM : Earth Observing System-Morning
EOS-PM : Earth Observing System-Afternoon
EUMETSAT : European Organisation for the Exploitation of Meteorological Satellites
MAST : Monterey Area Ship Track
MFO : Marine Fuel Oil
MOD06 : MODIS Cloud Product
MODIS : Moderate Resolution Imaging Spectroradiometer
NASA : National Aeronautics and Space Administration
QuickSCAT : Quick Scatterometer
SEVIRI : Spinning Enhanced Visible and InfraRed Imager
TIROS : Television Infrared Observations Satellite

LIST OF TABLES

Page

LIST OF FIGURES

Page

DETECTING SHIP TRACKS and ESTIMATING THEIR MICROPHYSICAL PROPERTIES in the ATMOSPHERE WITH MODIS DATA

SUMMARY

In this study, 1 km Moderate Resolution Imaging Spectroradiometer (MODIS) observations of morning (Terra) to afternoon (Aqua) passes were analyzed to estimate the particle sizes (and their changes in time) change of the aerosols that formed the ship tracks. Ship tracks are the low-level anthropogenic clouds that form around the exhaust released by ships. They modify the overlying cloud albedo by having high particle concentration and small droplet size and thus can be detected in near infrared imagery as bright features comparing to its surrounding. 2.13 μm observations are used for detecting ship tracks due to the large difference in the reflection from sea surface and ship exhaust. The MOD06 cloud algorithm is used to estimate effective particle radius change with time. Five case studies in different parts of the world are studied to examine the microphysical changes of the ship exhaust plumes in time. Ship track pairs were chosen both in Terra and Aqua MODIS imageries to estimate the particle size change from morning to afternoon time period. Particle size increased with time in the atmopshere as measured by distance from the ship. Particle growth over time is estimated to be up to 1 μm per hour. Terra and Aqua MODIS particle size estimates were in good agreement and both had particle size increasing with time. Terra and Aqua MODIS results are found to be 90±8% correlated with each other. The five case studies further demonstrated stability of the MOD06 algorithm.

ATMOSFERDEKİ GEMİ İZLERİNİN BELİRLENMESİ ve MİKROFİZİKSEL ÖZELLİKLERİNİN MODIS VERİSİ ile HESAPLANMASI

ÖZET

Bu çalışmada gemi izlerini oluşturan parçacık boyutunun 1 km çözünürlüğü olan MODIS datası ile sabah (Terra) geçişinden öğleden sonra (Aqua) geçişine kadar olan zaman dilimi içindeki değişimi analiz edildi. Gemi izleri, gemilerin egzosundan yayılan parçacıkların etrafında oluşan alçak seviyeli antropojenik bulutlardır, yani doğal yollardan değil, insan kaynaklı emisyonlar sonucu oluşurlar. Bu bulutları oluşturan parcacıklar sayı bakımından fazla, boyut bakımından küçük oldukları için, üstlerinde bulunan bulutları modifiye ederek yansıtma özelliklerini (albedo) değiştirirler ve bu sayede yakın kızılötesi görüntüde çevrelerinden daha parlak görünerek ayırd edilirler. Deniz yüzeyi ile gemi egzosu arasındaki yansıma özellikleri farkı, yani kontrastı, MODIS sensörünün 2.13 μm bandında daha büyük olduğu için, gemi izlerinin belirlenmesinde 2.13 μm kullanildi. Parçacıkların zaman içinde değişimini incelemek için MOD06 bulut algoritmasından yararlanıldı. Gemi emisyonu sonucu yayılan parçacıkların mikrofiziksel değişimlerini incelemek üzere değişik bölgelerden 5 lokasyon seçildi ve 5 durum çalışması yapıldı. Terra ve Aqua MODIS arasındaki zaman farkı içindeki parçacık değişimini hesaplamak için Terra ve Aqua MODIS sensörüne ait görüntülerde gemi izi çiftleri bulunarak, bu çiftlerinin karşılaştırılması yapıldı. Partikül boyutunun zaman geçtikçe ve kaynaktan uzaklaştıkça arttığı gözlendi. Partikül boyutunun zaman içindeki değişiminin 1 μm/saat'e kadar olduğu hesaplandı. Terra MODIS ve Aqua MODIS'in birbirleriyle uyum içinde olduğu ve her ikisinin de artan eğilim içinde oldukları gözlemlendi. Terra ve Aqua MODIS verisinde seçilen gemi izi çiftlerinin arasindaki korelasyon % 90±8 olarak hesaplandı. Seçilen 5 durum çalışmasının algoritma ile kararlılık gösterdiği sonucuna varıldı.

1. INTRODUCTION

The effect of anthropogenic aerosols on Earth's energy budget is an important issue for understanding changes in the global climate. Their effect can either be direct through scattering, absorbing and reflecting the incoming solar and infrared radiation or indirect by acting as a cloud condensation nuclei (CCN) which affects cloud droplet concentration and changes the cloud albedo (Arakawa, 2007). The Monterey Area Ship Track Experiment (MAST experiment) shows that ship tracks provide a good opportunity to understand the effect of man made aerosols in modifying the cloud reflectivity and hence the earth radiation balance (Durkee et al., 2000a).

Ship tracks, which were first observed by the TIROS VII satellite (Television Infrared Observation Satellite) in 1965 (Conover, 1966), are linear clouds seen in near-infrared images of marine stratocumulus that are caused by emissions from ships (Segrin et al., 2007). The MAST experiment team defines ship tracks as a bright curvilinear feature in near-infrared satellite imagery that is observed downwind of ship (Durkee et al., 2000a). Ship tracks occur in specific geographical regions of the globe and not every ship causes a ship track (Durkee et al., 2000b). In his work "Anomalous Cloud Lines", Conover defines the atmospheric conditions related to form a ship track as 1) a well mixed unstable layer from the surface to a low-level stable layer, 2) small changes in temperature and relative humidity at the surface, and 3) a small number of cloud forming nuclei (1966).

Clouds have the most significant influence on radiative energy exchange in the atmosphere (Arking, 1991). Since "ship tracks" are low level man made clouds, they also have an influence on global energy budget. Moreover, they provide a good example of cloud albedo modification and human impact on climate. In 1994, Platnick and Twomey used ship tracks to define cloud susceptibility and explained how the increase in cloud droplet number also increases the cloud reflectivity (albedo). The exhaust released by ship, which is anthropogenic pollution, increases the number of cloud droplets while reducing the droplet size (Coakley et. al., 1987) and thus eventually contributing to a cooling effect on earth's surface (Albrecht,

1989). Smaller droplet size also reduces the efficiency of droplet growth by collisions, thus suppresses drizzle (Ferek et al., 2000).

In this study, ship tracks and their microphysical properties are studied in the five case studies. MODIS (The Moderate Resolution Imaging Spectroradiometer) cloud products (MOD06) along with 1.6 μm, 2.1 μm, and 3.7 μm MODIS spectral band measurements from the Aqua and Terra satellites are used to estimate particle size change over time. MOD06 combines infrared and visible techniques to determine both physical and radiative cloud properties; it contains cloud-particle phase (ice vs. water, clouds vs. snow), effective cloud particle radius, and cloud optical thickness properties. Effective cloud particle radius for both Aqua and Terra satellites are used to guide the development and validation of this project.

2. SHIP TRACK CHARACTERISTICS

2.1 Ship Track Formation and Background Environmental Conditions

Direct atmospheric aerosol effects such as scattering and absorbing the solar radiation, and indirect aerosol effects from changing the microphysical properties of clouds have an important role on determining the Earth's energy budget. Indirect effect of aerosols, the so-called effect of anthropogenic aerosol, also changes the reflectivity of clouds when they act as cloud condensation nuclei (CCN) and form cloud droplets (Chuang and Penner, 1995). The "Ship Track" phenomenon is an interesting example that helps to understand how human-produced aerosols modify cloud albedo, and thereby the earth's energy budget. "Ship Tracks" are long-lived, curvilinear, brighter features observed on the near infrared satellite images downwind of ships (Conover 1966; Ackerman et al., 2000; Segrin et al., 2007).

NASA scientists describe ship tracks as clouds that form around the exhaust released by ships into the still ocean air. Water molecules attach to the aerosols released from the exhaust and form cloud seeds. Water vapor collects on the seeds until a visible cloud is formed. The cloud seeds are stretched over a long narrow path away from the ship due to wind and ship motion, and thereby ship tracks appear as long cloud strands over the ocean.

Ship tracks basically form in the low stratus and stratocumulus clouds off the western coasts of large continents. Stratiform clouds, on the other hand, form in the summer time when the subtropical high is fully developed (Evans, 1992). The dominant areas for stratiform cloud formation are the eastern ocean basins between 20° and 50° latitude (off the western coasts of continents), and at high latitudes above about 60° N and S (Durkee et al., 2000a). Schreier et al. (2007) also found ship tracks in the sub-tropical latitudes along the west coasts of southern Africa, South America, and North America in AATSR data. In these regions, cold upwelling ocean currents cause a stable atmospheric layer due to the northerly winds along the coast. This causes the marine boundary layer to saturate and thus provides an ideal environment

for the formation of statiform clouds (Evans, 1992). The formation of ship tracks is a result of a ship passing under the stratiform cloud. When the particles enter a stratiform cloud layer in the boundary layer, they either modify the existing cloud or they act as a CCN and form cloud droplets (Hobbs et al., 2000).

The boundary layer depth is also important for ship track formation. Ship tracks rarely occur in low-level clouds having altitudes more than 1 km; hence the low-level clouds must be close enough to the surface for ship tracks formation. A small rise in low-level cloud altitude affects the appearance of ship tracks and explains why they appear one day and disappear another day (Coakley et al., 2000). On the other hand, in their study, Durkee et al. (2000b) could not find any tracks at boundary layer heights greater than about 800 m, due to the reduction of ship-generated aerosols, and therefore smaller CCN concentrations in deeper boundary layers. Another thing affecting ship track disappearance is the cloud droplet size in the tracks. Cloud droplets grow to match the average droplet size in the cloud until the albedo of the ship tracks reaches to the surrounding cloud albedo (Durkee, 2000a).

Not every ship produces a ship track. An ambient condition is necessary in the marine atmosphere before ship track formation. Conover (1966) stated that conditions should include;

- Well mixed boundary layer from surface to a low level stable layer
- Low number of CCN
- Relatively small changes at surface temperature and relative humidity values

In addition to the ambient marine atmospheric conditions, the fuel burned by the ship also plays a significant role for ship track formation and particle emission (Hobbs et al., 2000).

2.2 Ship Track Effects on Climate

Particles emitted from ships may directly affect the marine atmosphere in several ways. Low clouds over the large open seas have fewer CCN than clouds over land; hence, they have larger droplet radii for similar water content and dispersion of droplet size distributions. Ship track clouds contain more CCNs with smaller mean

droplet radii than surrounding clouds (Schreier, 2006). With fewer droplets, the albedo of marine clouds is more sensitive to changes in droplet number concentration. Since water molecules collect around an aerosol particle to form a droplet, cloud albedo depends on aerosol particle number and size distribution (Öström, 2000). Increased aerosol concentrations can produce higher droplet concentrations and thereby enhance cloud albedo (Twomey effect) due to small particle reflection (Ackerman et. al., 2000). More reflective clouds are associated with smaller particles with high cloud albedo, which bounce sunlight back into space and cool the planet (Albrecht, 1989).

The term "Cloud Susceptibility" also refers to the CCN influence on cloud albedo. It can be defined as the sensitivity of cloud albedo to changes in cloud droplet concentration (Platnick and Twomey, 1994). Clouds that have many but small droplets are less susceptible to increases in CCN than clouds that are geometrically thin with few but large droplets (Coakley et al., 2000). Platnick and Twomey (1994) show that clouds within ship tracks are less susceptible to CCN increases than clouds outside of ship tracks.

Another influence of CCN concentration is the change of the drizzle process. Drizzle is a rain precipitation containing droplet sizes larger than cloud droplets but smaller than raindrops. Droplets may grow in clouds firstly by condensation, afterwards by collision and coalescence of droplets. Since the ship tracks have fewer droplets in collision-coalescence size range, they are less likely to produce drizzle-size droplets, in contrast to ambient clouds where drizzle-size droplets are often present (Ferek et al., 2000). High droplet concentrations and small particle sizes suppress the growth of large particles by collision and ultimately the occurrence of drizzle. Liquid water content in the ship track increases because the higher droplet concentrations and the smaller droplet sizes limit the loss of liquid water by precipitation (Radke et al., 1989).

2.3 Detecting Ship Tracks in Visible and Near-Infrared Imagery

Although ship tracks can be observed in both visible and near-infrared imagery, many more ship tracks appear in the near infrared (Durkee et al., 2000a). Cloud droplets, cloud droplet size, optical thickness, and liquid water path are deduced from solar reflection measurements in non-absorbing visible and absorbing near-

infrared spectral bands. Visible reflectance contains optical thickness information and near-infrared reflectance specifies particle size; thus the typical absorbing channels at 1.6, 2.13, and 3.75 μm are used to detect aerosol properties (Platnick et al., 2000). Figure 2.1 shows cloud spherical albedo as a function of wavelength for different values of the particle sizes.

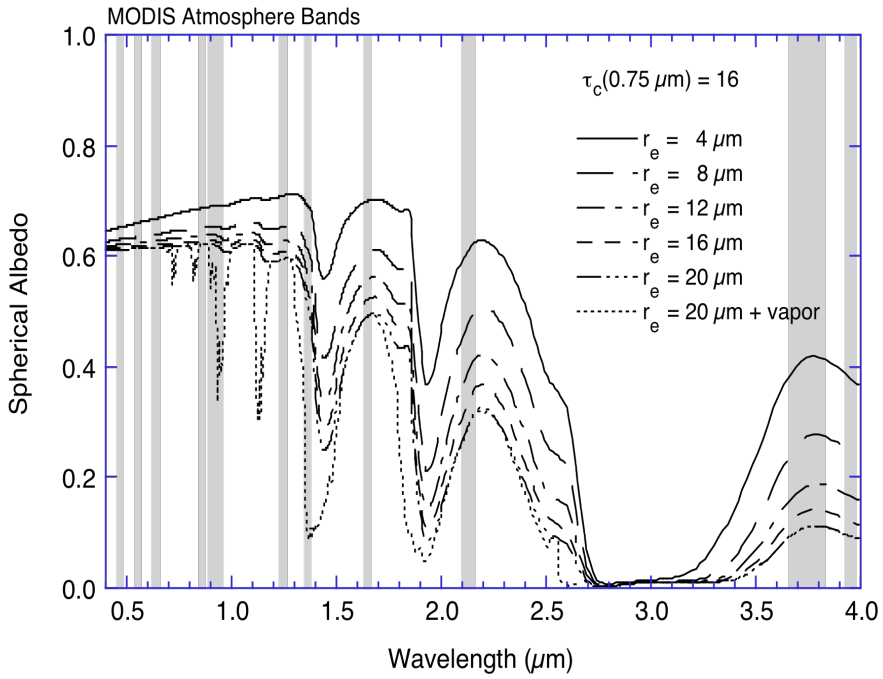

Figure 2.1 : Cloud spherical albedo as a function of wavelength for various values of the effective radius (King et al., 1997)

Spherical albedo represents global albedo over all sun angles (King et al., 1992). For a given optical thickness, clouds with larger droplets reflect less in near infrared wavelengths, so they have smaller albedo values (Platnick et al., 2000). Ship tracks, on the contrary, contain particles with smaller effective radius, compared to those in the near vicinity. Thus, they reflect more and have higher albedo values. Ultimately, at near-infrared wavelengths, ship tracks appear as bright lines that can be distinguished from the surrounding features. Figure 2.2 shows this inverse relationship between effective radius and reflectance at 2.13 μm. The first, second and the third plumes are shown in blue, red and green colors, respectively.

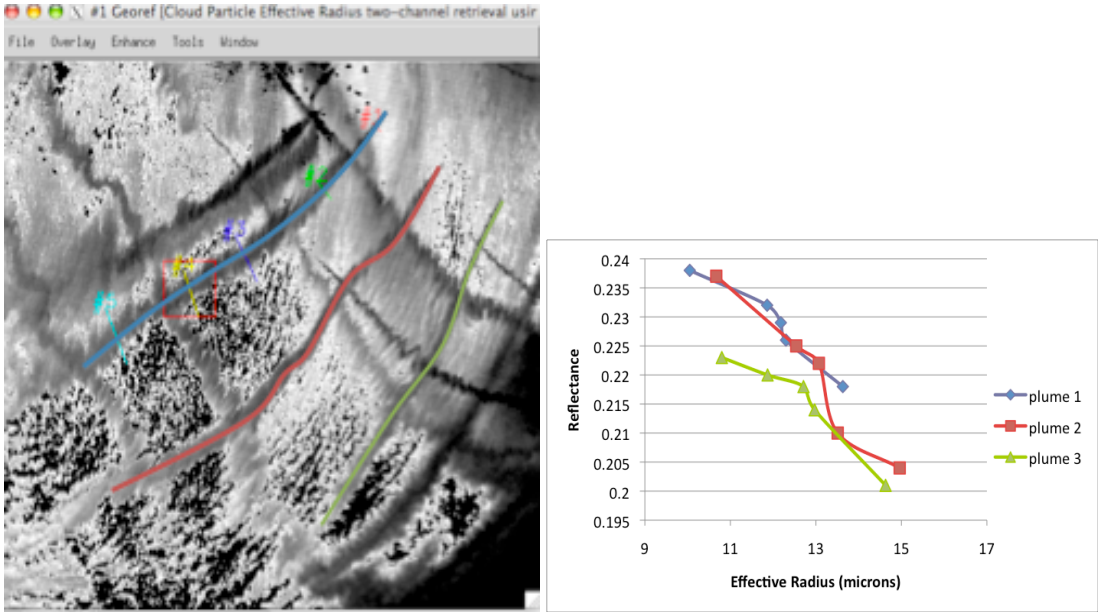

Figure 2.2 : Inverse relationship between effective radius and reflectance at 2.13 µm.

As demonstrated in Figure 2.2, as the particle size gets bigger the reflectance values get smaller. In ship tracks, the particles are so small and they do not collide enough to reach droplet size. Since drizzle is suppressed, the liquid water content in the cloud increases (Albrecht, 1989). This also makes the cloud brighter and more reflective to incoming sunlight, especially in the near-infrared part of the spectrum due to the small water vapor absorbtion at 1.64 µm and 2.13 µm (King et al., 1992). These wavelenghts can be used to discriminate small particles from big ones.

2.4 Ship Impacts on Ship Track Formation

Another important factor for determination of ship track characteristics is the ship itself. Fuel type is an important factor in determining whether the ship will produce a ship track or not (Hobbs et al., 2000).

Commercial ships are powered either by diesel engines or steam turbine engines. Diesel powered engines burn cheap, low-grade fuel, known as marine fuel oil (MFO) while steam-powered engines burn higher grade fuel. Diesel-powered engines using MFO emit greater numbers of particles than turbine-powered engines using navy distillate fuel (Hudson et al., 2000). Ships burning MFO emit particles with a larger radius than those burning navy distillate fuel. For the same ambient conditions, ships burning MFO are more likely to form ship tracks than ships burning high grade

distillate fuel, since engines burning MFO emit numerous particles large enough to serve as CCN. (Hobbs et al., 2000).

In steam turbine engines, the fuel is combusted at higher temperatures than in diesel powered engines. Thus, in steam turbine engine the fuel burns faster and more completely and there are fewer unburned gaseous hydrocarbons in the exhaust. Ultimately, due to the high temperature of combustion in steam or gas turbine engines, they release smaller particles. The main difference between diesel powered engines and other internal combustion engines is that they auto-ignite and therefore produce high particulate emissions. Nuclear powered ships, on the other hand, emit heat but negligible particles, thus they do not produce ship tracks since water vapour and heat emissions do not play an important role in ship tracks formation (Hobbs et al., 2000).

Ship tracks from diesel ships are longer, older, and wider than ship tracks from steam turbine ships. Also ships that produce more aerosol, such as diesel powered ships burning MFO, produce ship tracks that are not only brighter especially at near-infrared wavelengths, but also wider, and longer-lived than do ships that produce less aerosol (Durkee et al., 2000b).

3. DATA USED

3.1 MODIS Data Overview

MODIS (Moderate Resolution Imaging Spectro-radiometer) is a 36 spectral band scanning radiometer on board the Terra (EOS AM) and Aqua (EOS PM) satellites. It has a long-term science data supply mission, so as to develop scientists' knowledge about global changes on the land, in the oceans, and in the lower atmosphere. Those 36 MODIS bands, whose band characteritics are summerized in Table 3.1, provide worldwide data sets every 2 days from a polar-orbiting, sun synchronous, platform at an altitude of 705 km with a 2330 km swath width.

Table 3.1 : MODIS bands and their principle areas of application.

Band	Wavelength (nm)	Resolution (m)	Primary Use
1	620-670	250m	Land/Cloud/Aerosols Boundaries
2	841-876	250m	
3	459-479	500m	Land/Cloud/Aerosols Properties
4	545-565	500m	
5	1230-1250	500m	
6	1628-1652	500m	
7	2105-2155	500m	
8	405-420	1000m	Ocean Color/ Phytoplankton/ Biogeochemistry
9	438-448	1000m	
10	483-493	1000m	
11	526-536	1000m	
12	546-556	1000m	
13	662-672	1000m	
14	673-683	1000m	
15	743-753	1000m	
16	862-877	1000m	
17	890-920	1000m	Atmospheric Water Vapor
18	931-941	1000m	
19	915-965	1000m	

Band	Wavelength (μm)	Resolution (m)	Primary Use
20	3.660-3.840	1000m	Surface/Cloud Temperature
21	3.929-3.989	1000m	
22	3.929-3.989	1000m	
23	4.020-4.080	1000m	
24	4.433-4.498	1000m	Atmospheric Temperature
25	4.482-4.549	1000m	
26	1.360-1.390	1000m	Cirrus Clouds Water Vapor
27	6.535-6.895	1000m	
28	7.175-7.475	1000m	
29	8.400-8.700	1000m	Cloud Properties
30	9.580-9.880	1000m	Ozone
31	10.780-11.280	1000m	Surface/Cloud Temperature
32	11.770-12.270	1000m	
33	13.185-13.485	1000m	Cloud Top Altitude
34	13.485-13.785	1000m	
35	13.785-14.085	1000m	
36	14.085-14.385	1000m	

36 spectral bands acquire data at three spatial resolutions: 250 m for 2 bands, 500 m for 5 bands, and 1000 m for 29 bands. These bands have been carefully selected to improve scientist's understanding about global dynamics of land, ocean, and atmospheric processes (King et al.,1992).

Four of these bands are used in a daytime cloud properties algorithm over the land; they are in the visible (0.645 μm) and near infrared (1.64, 2.13, and 3.75 μm) spectral regions. Thermal bands, such as the 8.55, 11.03, 12.02, 13.335, 13.635, 13.935 and 14.235 μm are used to infer cloud cover and cloud top properties (including cloud top altitude, cloud top temperature and thermodynamic phase). Finally 0.645, 2.13 and 3.75 μm bands are used to retrieve the cloud optical thickness and effective particle radius over land. (0.858 μm band is used instead of 0.645 μm over ocean) (King et al., 1997).

There are many standard MODIS data products available for scientists to study global change in the atmosphere, land, ocean, and cryosphere. The MODIS cloud product (MOD06) will be used to examine ship emitted particle effective radii and their changes.

3.2 MODIS Cloud Product (MOD06 Algorithm)

The MOD06 cloud algorithm uses both emitted thermal radiation measurements and reflected solar measurements. This algorithm can basically be applied to plane-parallel liquid water clouds. It presents information regarding the optical and thermo dynamical properties of cloud layers, optical thickness, effective particle radius, and particle phase. Using 1-km resolution MODIS visible, near-infrared, and shortwave infrared bands, cloud particle phase, effective radius, cloud optical thickness, and cloud integrated water path are derived. Other cloud properties such as, cloud top temperature, cloud top pressure, effective emissivity, and cloud particle phase are produced by infrared retrieval methods (King et al., 1997).

Aerosol effective radius is defined as an area weighted mean radius of the aerosols. Aerosol Optical Thickness is the degree to which aerosols inhibit the transmission of light (NASA, Goddard Earth Sciences, 2009). According to the ATBD (Algorithm Theoretical Basis Document), the studies of the determination of cloud optical thickness and/or effective particle radius are based on the reflection function. In non-absorbing visible spectral bands, the reflection function is a function of optical thickness, whereas in near infrared water (or ice) absorbing spectral bands, it is a function of cloud particle size. The reflection function R (τ_c, r_e; μ, μ_0, φ) represents the albedo of the ambient, which is formed from a ratio of the reflected intensity I(0, - μ, φ) and the incident solar flux density, and is defined by;

$$R(\tau_c, r_e; \mu, \mu_0, \phi) \equiv \frac{\pi \, I(0, -\mu, \phi)}{\mu_0 F_0} \qquad \textbf{(3.1)}$$

where τ_c is the total optical thickness of the atmosphere (or cloud), r_e is the effective radius of the particle, μ_0 is the cosine of the solar zenith angle, μ the absolute value of the cosine of the zenith angle, measured with respect to the positive τ direction, and φ the relative azimuth angle between the direction of propagation of the emerging radiation and incident solar direction (Nakajima and King, 1990). The reflection function does not depend on the cloud particle size distribution but it does depend on effective radius. For the near infrared bands, the reflectance of a cloud decreases with the increasing particle size (King et al., 1997). A wide variety of solar zenith, observational zenith, and azimuth angles must be accounted for in the radiative transfer calculation at selected wavelengths in both visible and near infrared in order to evaluate the cloud particle effective radius.

Figure 3.1 shows the representative reflection function calculation presented in the ATBD; it illustrates the basic principle of determination of the effective radius and optical thickness from reflected solar radiation measurements (King et al., 1997). Spectral bands at 0.664 and 1.621 μm were chosen since they are outside of water vapor and oxygen absorption bands and have different water droplet absorption characteristics.

The dashed curves in the figure represent the reflection functions for certain values of the cloud optical thickness while the solid curves represent the reflection functions for specified values of the effective particle radius.

Figure 3.1 shows that the reflection function at a non-absorbing wavelength (0.664 μm) is mostly used for cloud optical thickness determination, with a little dependence on particle radius. On the other hand, the reflection function at 2.142 μm (or 1.621 μm) is useful for determination of the effective radius with little dependence on cloud optical thickness. In other words, the maximum reflection function at 2.142 μm generally occurs for smaller effective radius values, depending on optical thickness.

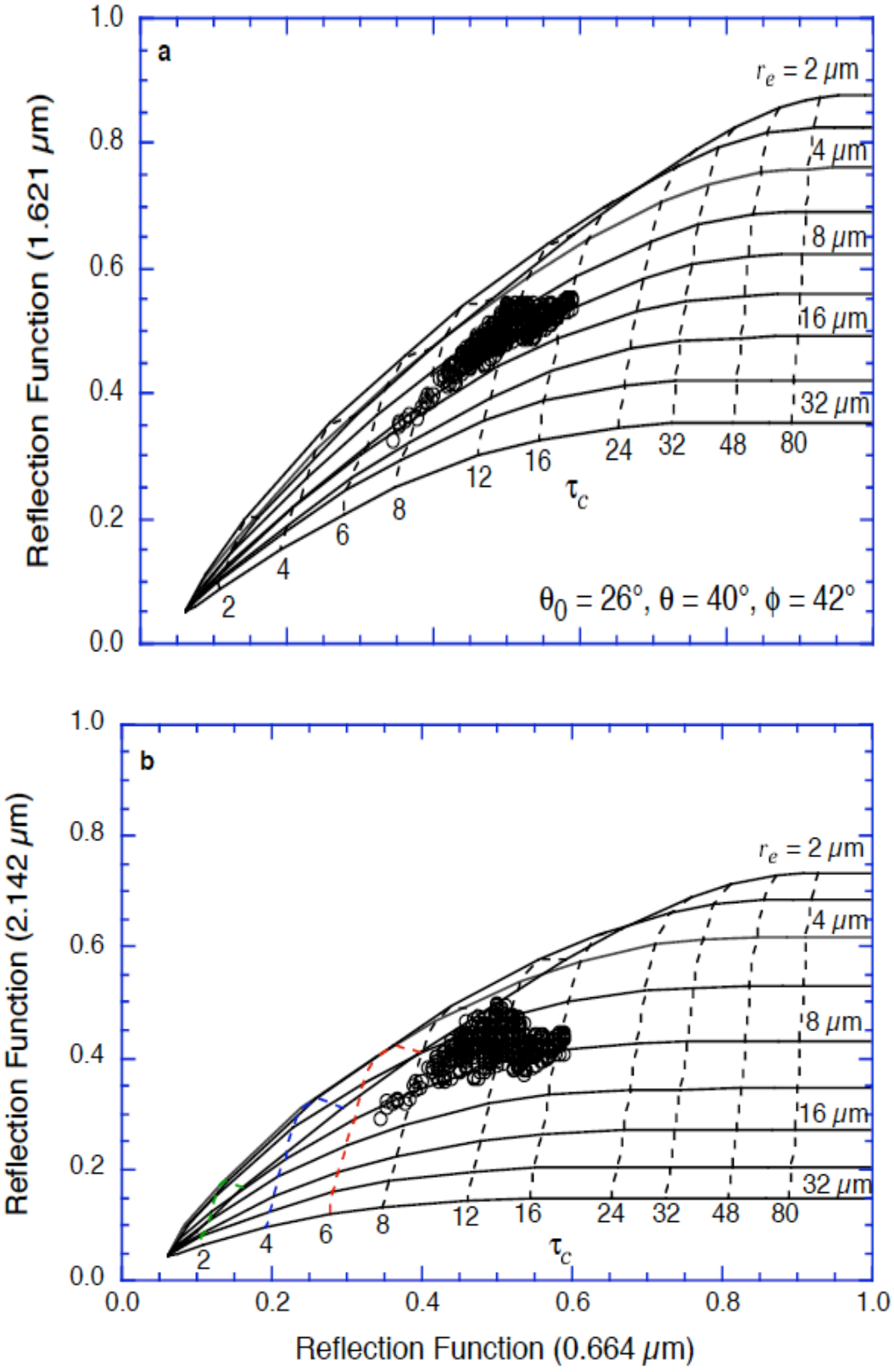

Figure 3.1 : Theoretical relationship between the reflection function at 0.664 and (a) 1.621 μm and (b) 2.142 μm for values of optical thickness (at 0.664 μm) and effective radius when solar zenith angle θ_0=26°, observational zenith angle θ=40° and azimuth angle φ=42° (King et al., 1997).

The size of the droplet makes ship tracks brighter than the marine cloud layer. The incoming radiation is scattered from the surface of the droplets, so the scattered radiation is proportional to the total surface area of the droplets ($\sim r^2$) in a particular volume of cloud where the absorption of the radiation is proportional to the total volume of the droplets ($\sim r^3$) since it occurs inside the droplet. The ratio of the scattered radiation to absorption, which is the net radiation, is inversely proportional to the size of the droplet ($\sim r^{-1}$). Hence, clouds with smaller droplets reflect more infrared solar radiation and they seem brighter than the surrounding clouds. This dependence of the reflectance on droplet size is related to effective radius, which is the ratio of total volume of the drops to their total surface area (Rosenfeld and Woodley, 2001).

Figure 3.2 shows ship tracks in different wavelengths of the visible and near infrared spectral regions.

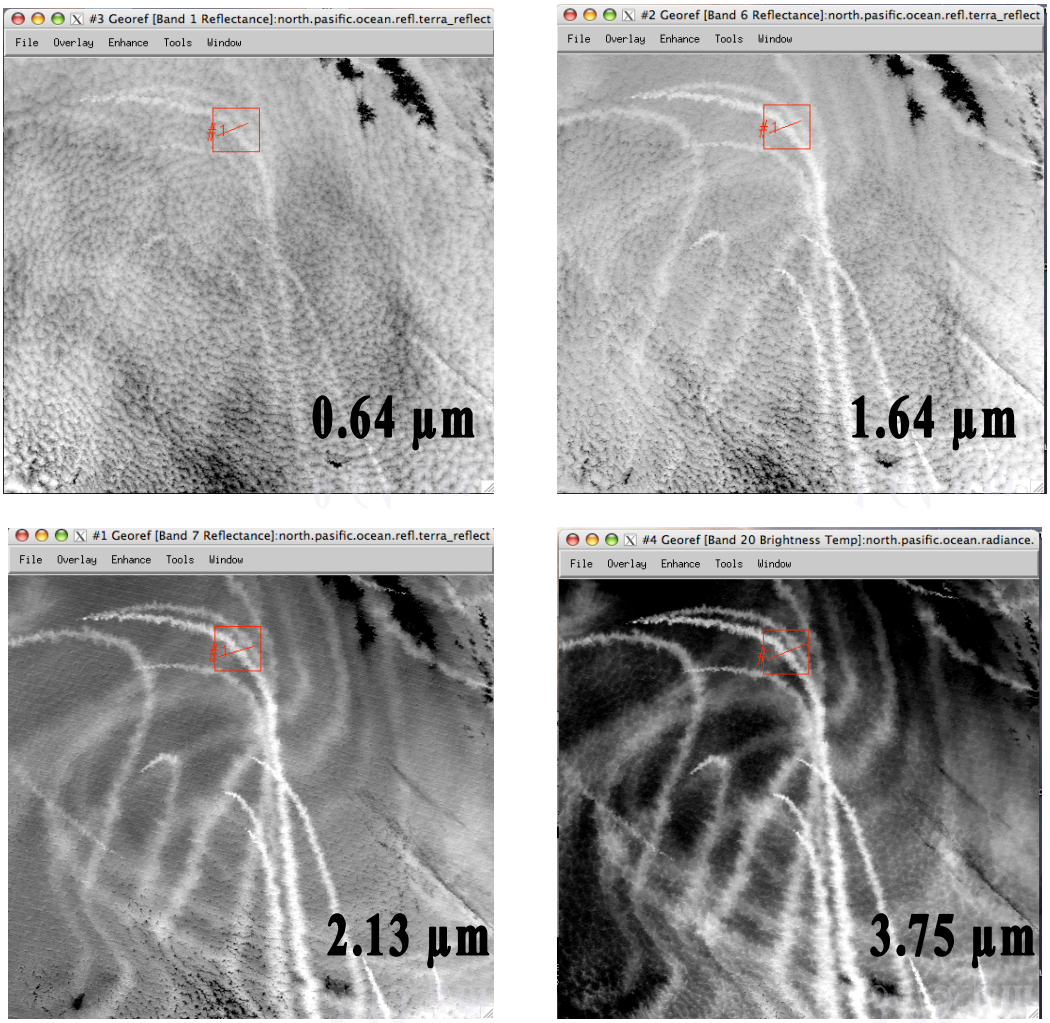

Figure 3.2 : Ship tracks in different wavelengths.

At the longer wavelengths, the ship track contrast increases. Visible wavelength (0.65 μm) is primarily a function of cloud optical thickness, whereas near-infrared wavelengths (1.64, 2.13, and 3.75 μm) are sensitive both to optical thickness and, especially, cloud particle size (Nakajima and King, 1990). Ship tracks are more apparent at longer wavelengths. 2.13 μm is very useful for determination of the effective particle radius as the difference in the reflection from sea surface and ship exhaust is the greatest.

The MOD06 algorithm is based on three different band combinations. Depending on the viewing angle, solar angle and liquid water content of the cloud, these three channels look at a different part of the cloud. 3.7 μm band sees the top of the cloud, 2.13 μm band sees middle part of the cloud, and 1.64 μm observes particles in the lower part of the cloud. For water clouds, since the effective radius of particle increases from cloud base to cloud top, 3.7 μm is sensitive to drops high in the cloud while 1.64 μm is sensitive to those in the lower part of the cloud (Straka III and Heidinger, 2006).

4. METHODOLOGY

4.1 Effective Radius Estimations

MODIS measurements at 1 km from the morning Terra and afternoon Aqua satellites are analyzed along with the MOD06 cloud product for five different locations around the world. The MOD06 effective particle radius product is studied to infer the particle size change as a function of time. ENVI is used as software for processing and analyzing geospatial imagery. The length of time that the portion of a ship track plume has been in the atmosphere is estimated from ship speed, wind speed, and distance along plume (from the ship location). Effective radius change over time estimates are made from MOD06 determinations along a transect perpendicular to the ship track, away from ship track intersections as shown in Figure 4.1.

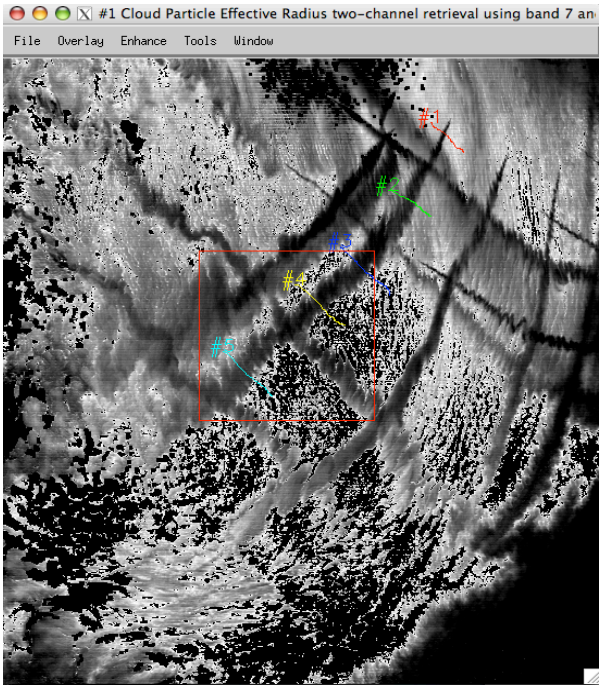

Figure 4.1 : Transects over a ship track.

Atmospheric parameters such as moisture and wind also affect ship track plume formation. When air is saturated with moisture, more water vapor collects on the cloud condensation nuclei (CCN). On the other hand, aerosols (e.g. cloud seeds) are

stretched over a long, narrow path according to the direction of the wind.

QuikSCAT (Quick Scatterometer) data is used for estimation of wind speed and direction. The wind map is acquired from Seawinds, which is attached to QuickSCAT. It is microwave radar and measures near-surface wind speed and direction (Remote Sensing Systems). Moisture is estimated using data from AMSR-E (Advanced Microwave Scanning Radiometer for EOS) on board the Aqua satellite (NASA/Marshall Space Flight Center).

4.2 Vessel Speed Calculations

The displacement between initial ship exhaust location and subsequent along track position depends not only on the wind direction but also on the propulsion of the ship (Christensen, 2008). A Haversine formula is used to calculate the distance between ship locations in the Terra and Aqua images. The Haversine formula, an equation important for navigation, is based on the great-circle distance, which is the shortest distance between any two points over the Earth's surface. It is given by;

$$\begin{aligned} \Delta lat &= lat_2 - lat_1 \\ \Delta long &= long_2 - long_1 \\ a &= \sin^2(\Delta lat/2) + \cos(lat_1)\cos(lat_2)\sin^2(\Delta long/2) \\ c &= 2a\tan 2\left(\sqrt{a}, \sqrt{(1-a)}\right) \\ d &= Rc \end{aligned} \qquad \textbf{(4.1)}$$

R refers to earth's radius (mean radius = 6371km), "c" is the angular distance in radians, and "a" is the square of half the chord length between the points (Movable type scripts, 2010).

Earth located Aqua and Terra MODIS imagery reveal the latitude and longitude values that are used to find the distance that the ship traveled. Figure 4.2 shows the distance calculation between Terra and Aqua. The distance can be calculated by Haversine formula, since the latitude/longitude values and the time difference between two sensors are known. In each of the five cases studied over different parts of the world, 4-5 plumes are chosen to investigate the tine evolution of the ship track plume effective cloud particle radius (which is estimated from MOD06 determinations along a transect perpendicular to the ship track, away from ship track intersections).

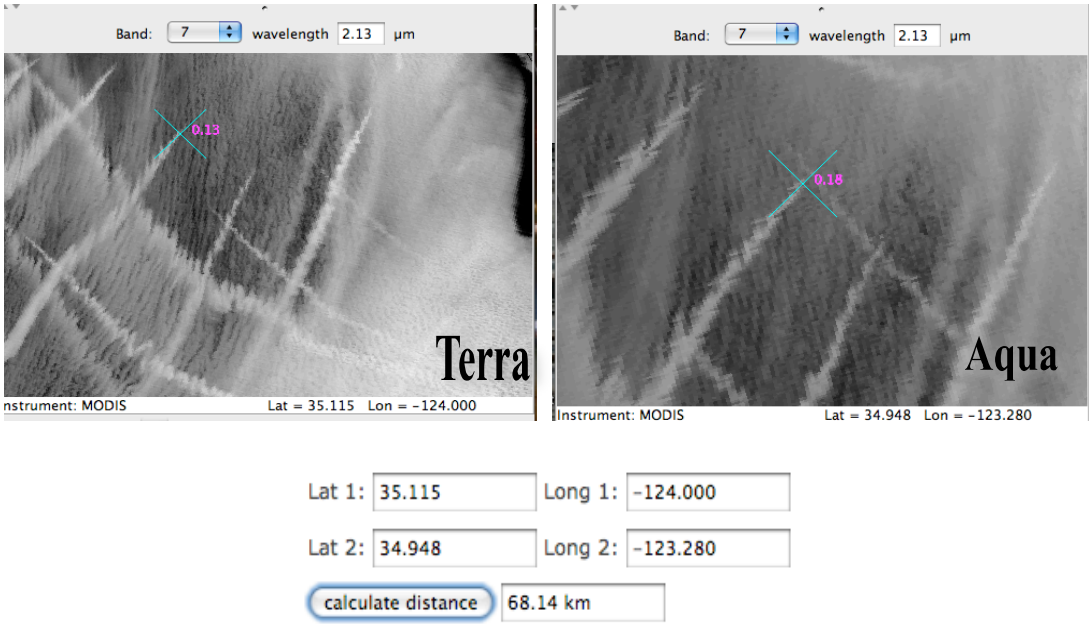

Figure 4.2 : Distance calculation between Terra and Aqua imageries.

Particle radius growth in time is shown for both Terra and Aqua MODIS imagery for the selected plumes and the results are then compared to each other. To do these comparisons, the Aqua MODIS data time series are interpolated to the Terra MODIS time series to obtain new effective radius values for Aqua in terms of Terra. These new effective radius values of Aqua are correlated with the effective radius values of Terra.

4.3 Spatial Resolution Sensitivity

In higher resolution imagery, more small scale features can be detected. MODIS obtains data with 250 m, 500 m and 1 km spatial resolution. MODIS data with 1 km spatial resolution data are used to examine the effective radius change over time for this study. Figure 4.3 shows how spatial resolution affects the features in the imagery.

Terra MODIS band 7, at 2.13 µm, is shown in different spatial resolutions to illustrate the reflectance change. More details with less coverage are shown at 1 km, while fewer details with larger coverage are shown at 4 km. The data values (in the plots on the right) indicate the reflectance in percentage along a transect perpendicular to the plume.

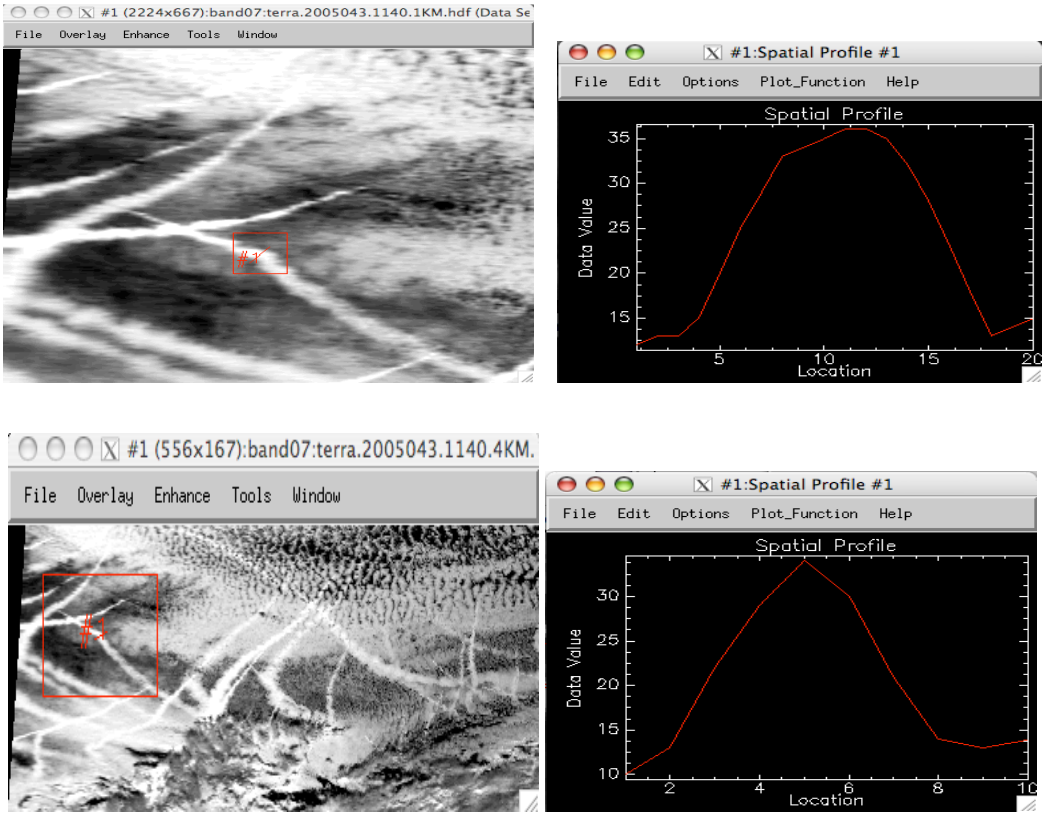

Figure 4.3 : Reflectance at 2.13 µm at 1 km (top) spatial resolution and 4 km (bottom) spatial resolution.

The reflectance values for the 1 km resolution transect are greater than values for 4 km resolution. The pixel extent of the transect as measured in high reflectance pixels decreases as resolution is decreased (e.g. at 1 km transect at half maximum values of reflectance extends approximately 10 pixels and at 4 km it extends approximately 4 pixels). As resolution decreases (e.g. at 5 km), plumes often become undetectable.

4.4 Ship Track vs. Non-Ship Track Case

It is mentioned that the ship tracks have smaller particle sizes and thus they reflect more incoming radiation back to the space. On January 10, 2008, MODIS captured a parallel rows of clouds line image over the Caspian Sea. In appearance, they look like ship tracks, which are usully in long, narrow linear shape, however those parellel cloud lines are called cloud streets. While ship tracks form around the particles released by ships, this horizontal roll vortices form when cold air blows over the warmer, moister air that sits over the water. Due to the wind direction, they line up like spinning straws

(NASA Earth Observatory). Since they are not anthropogenic clouds, their particle sizes are larger and thus their reflectivity is smaller comparing to ship tracks. Figure 4.4 show the reflctance values for the cloud streets.

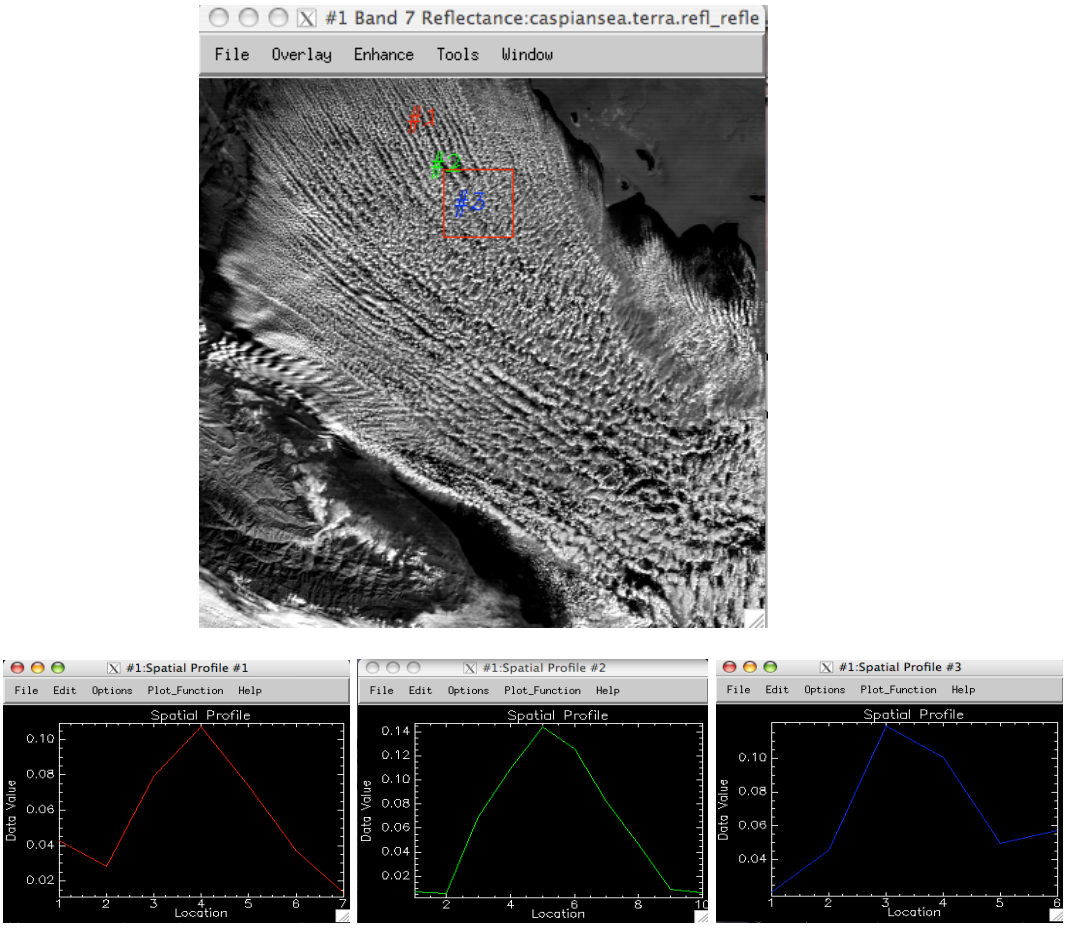

Figure 4.4 : Reflectance values of cloud streets.

Reflectance values at 2.13 μm is shown in Figure 4.4. The x-axis of the profiles show the length of the line, which is selected manually on the imagery, and the y-axis of the profiles show the reflectance values. As can be seen from the figure, the reflectance values are around 0.10 to 0.14, which is consistent with large particle reflectance case. However, the reflectance values of the ship track particles are larger due to the smaller particle size. Figure 4.5 shows the effective particle size of the cloud streets. The particle size is estimated from MOD06 MODIS cloud product. Four points are chosen randomly on the imagery and the results are shown accordingly.

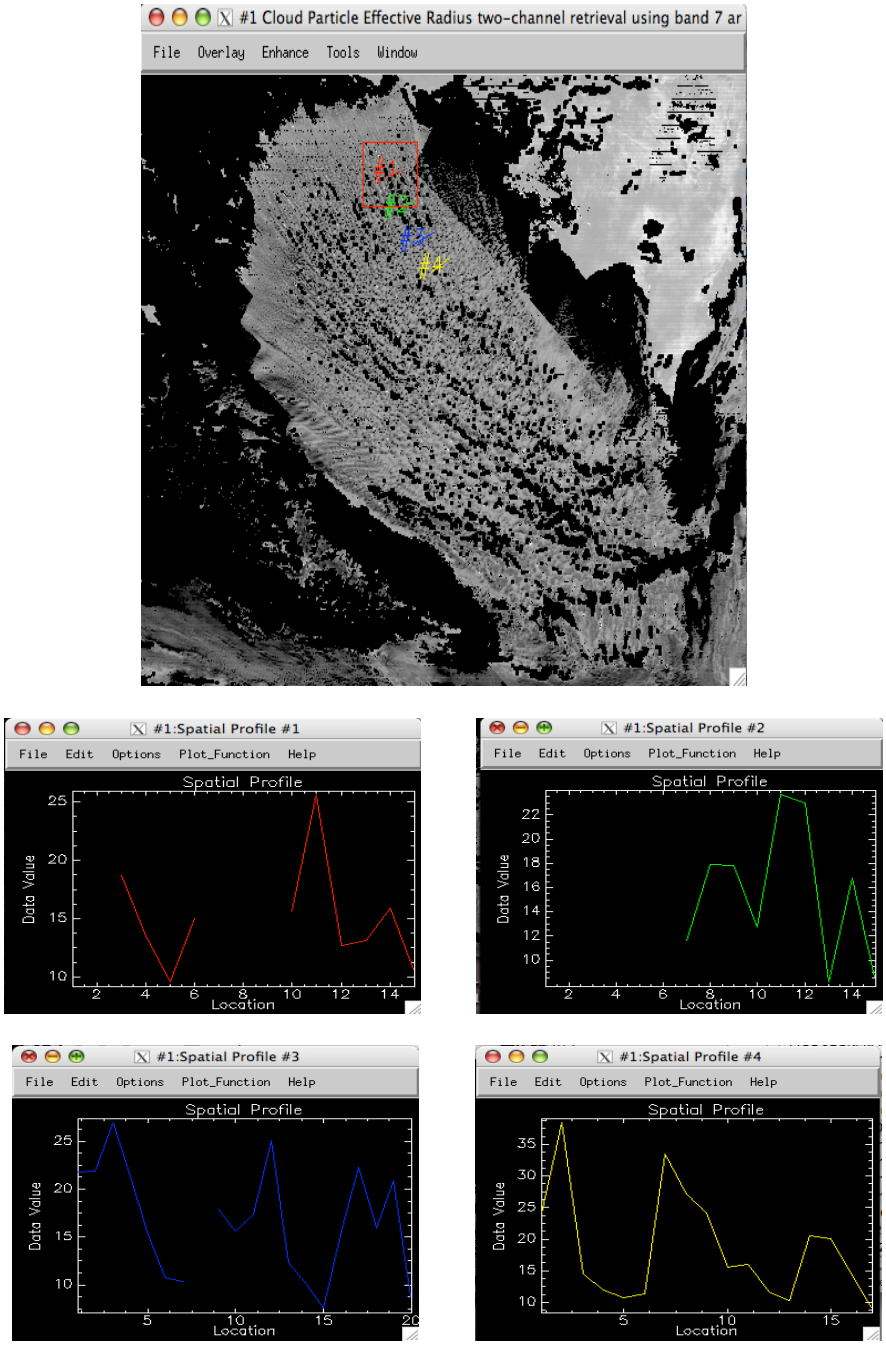

Figure 4.5 : Effective particle radius size for cloud streets.

Particle size values are more than 20 μm, which is almost two times larger of the particles those from ship tracks. This illustrates how particle size and reflectivity change in ship track and non-ship track situations.

5. CASE STUDIES

Particle size growth with time is estimated with MODIS Aqua and MODIS Terra data over five different part of the world. Case studies include;

1. California (September 30, 2005),
2. North Pacific Ocean (February 10, 2003),
3. Alaska (March 4, 2009),
4. Kuril Islands (July 2, 2003),
5. Europe Case (February 12, 2005)

5.1 California Case Study

Ship tracks were seen in satellite images off the coast of California on September 2005. These string like clouds form when the water molecules condense on the particles particles released from ship exhaust. Due to the wind direction, those particles stretch over a long, narrow path, and form as a string like clouds. Figure 5.1 shows the location of the ship tracks formation.

Figure 5.1 : Location of ship tracks of California Case.

Since the particles emitted by ship are smaller than those in the nearby atmosphere, their albedo is higher than the surrounding clouds. They seem brighter in the near infrared imagery due to their high reflectance. Figure 5.2 shows the reflectance

values for the ship tracks. Terra band 7 (2.13 µm) is chosen to display the reflectance values in and out of the ship tracks over the California coast.

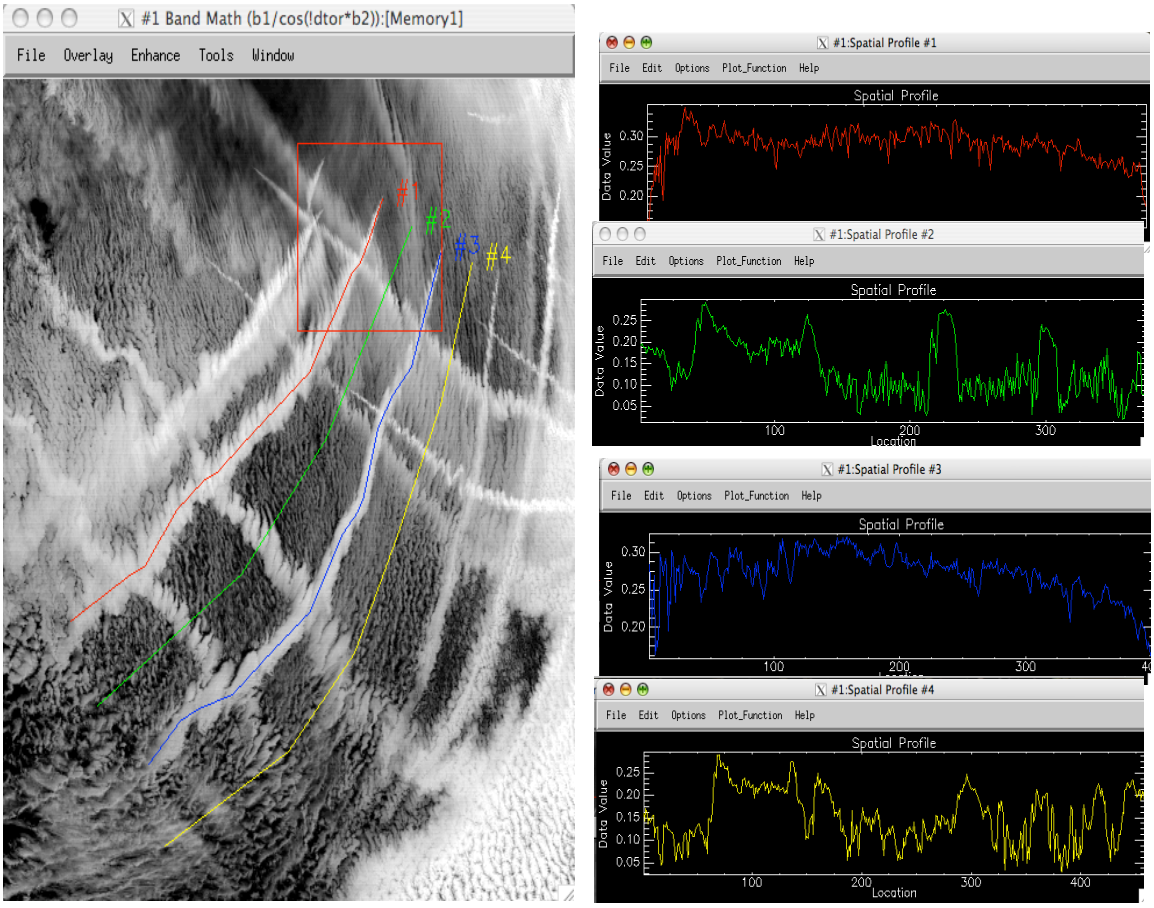

Figure 5.2 : Reflectance in and out of plume.

Red, green, blue, and yellow lines show the transects within and along-side the plumes and the values are shown respectively. The Y axis indicates the reflectance values for the chosen transects. The X axis indicates the location along the transect. The reflectance values within the plumes, which are shown in red and blue colors, are bigger (~0.30) than the values out of (along-side) the plumes, which are shown in green and yellow colors (~0.25). This illustrates how the smaller particles in the plumes reflect more than the particles surrounding the ship tracks. Thus, they can be discriminated from their vicinity in visible and especially in near infrared wavelength region. Ship tracks are more apparent as the wavelength gets bigger. 2.13 µm is very useful for determination of the effective particle radius as the difference in the reflection from sea surface and ship exhaust is the greatest.

Figure 5.3 shows the moisture map and wind map, which are important atmospheric

parameters for ship track formation.

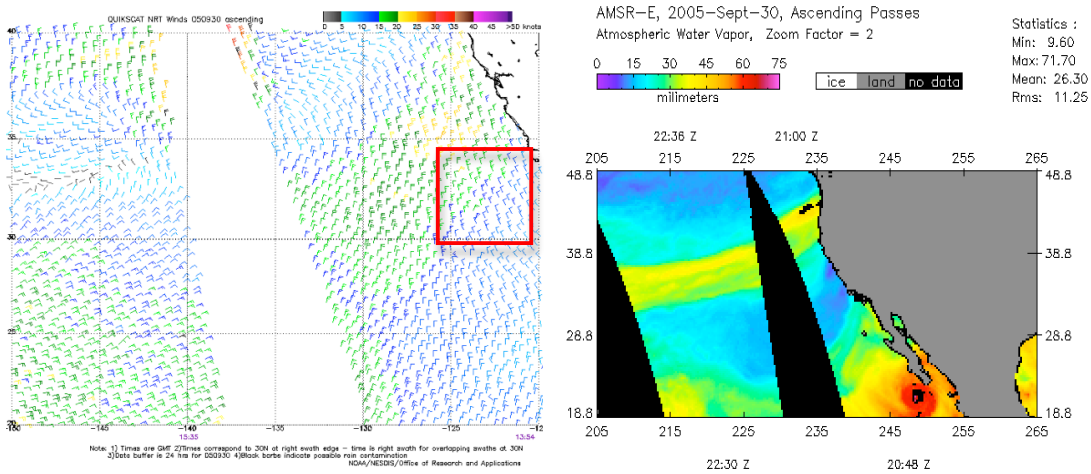

Figure 5.3 : Wind map and moisture map for California case.

Stratiform clouds are convenient for ship track formation and for stratiform cloud formation; not only a stable atmospheric layer, but also northerly wind is necessary. According to the wind map, the wind blows from the north with a speed of around 15 knots. According to the moisture map, the values are approximately 15 millimeters and there is no strong moisture gradient for the ship track area, which is one of the necessary ambient conditions in the marine atmosphere before ship track formation.

Terra MOD06 and Aqua MOD06 cloud algorithm data is used to investigate microphysical properties (e.g. particle effective radius) of ship tracks. Terra and Aqua datasets with 1 km resolution cover the same region with a time difference of 95 minutes. Cloud particle growth as a function of time is studied for five ship tracks in both datasets. The ship track cloud locations are chosen away from ship track intersections and cloud particle effective radius values are noted.

Figure 5.4 shows the effective radius change over time for Terra and Aqua data. The upper graphs represent all plumes selected for Terra and Aqua data separately, while the lower graphs represent their comparisons for each plume. The plume which is found on Terra MODIS imagery is also found on Aqua MODIS imagery, so the ship track pairs is identified. Thus, the comparison of Terra and Aqua MODIS is done according to the chosen ship track pairs.

Plume 1 is shown with blue color, plume 2 is shown with red color, plume 3 is shown with green color, plume 4 is shown with purple color and plume 5 is shown

with cyan color and the comparison graphs indicates the plumes accordingly.

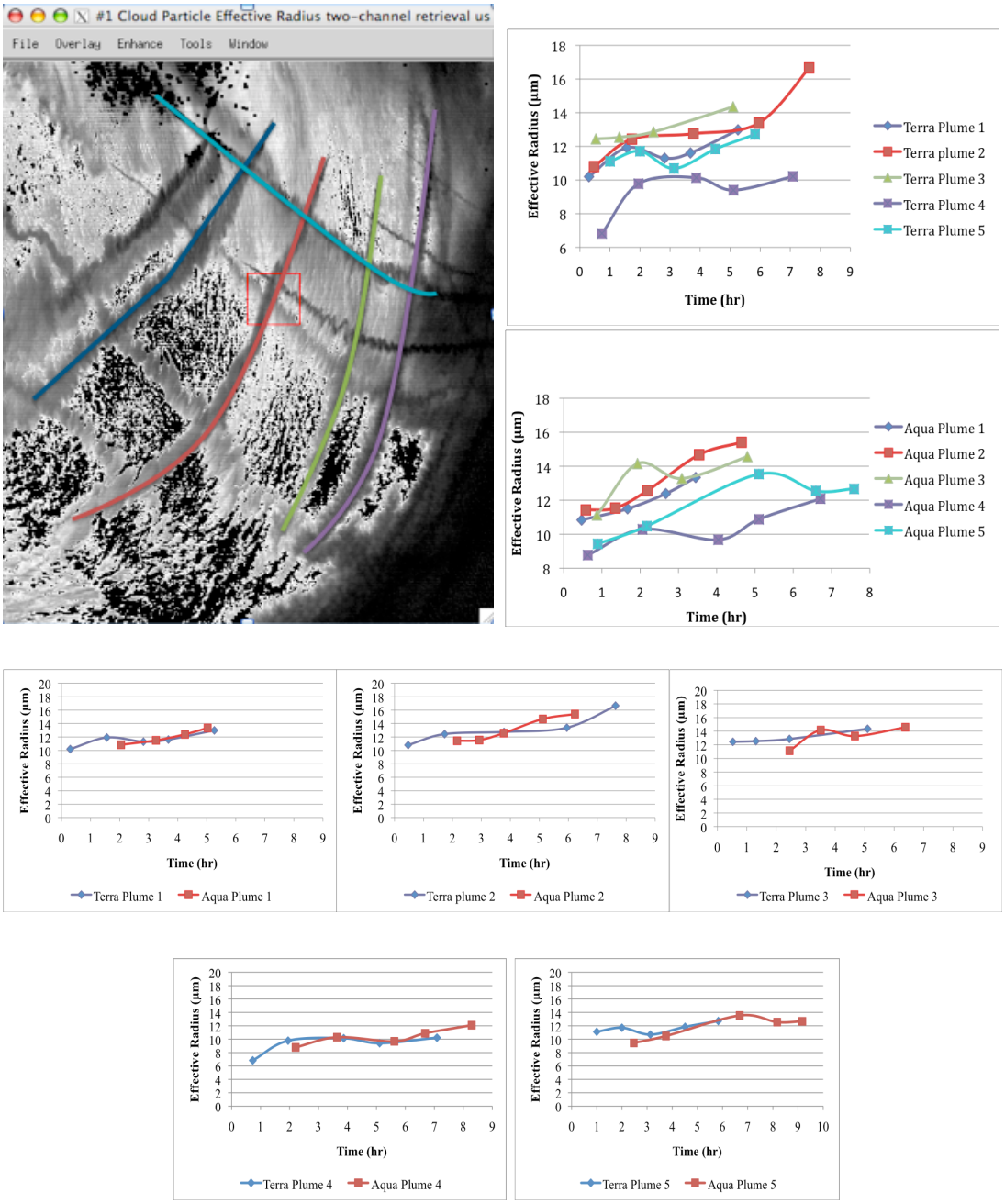

Figure 5.4 : Effective radius change with time for MODIS Aqua and MODIS Terra and their comparisons for each plume for California case.

The growth of the particle size (rate of change) is calculated to be between 0.3 to 0.8 µm per hour for Terra; 0.5 to 1.0 µm per hour for Aqua. Terra and Aqua partcle size estimates are compared against each other. Interpolation is used get a new effective radius for Aqua. The two sensor's effective radius values for each selected common plume are correlated with each other. It is noteworthy that Terra MODIS and Aqua MODIS determinations are in agreement with .86 to.98 correlation values.

5.2 North Pacific Ocean Case Study

The area over North Pacific Ocean, February 10, 2003 is chosen as another case to examine the microphysical cloud properties from ship emissions. Figure 5.5 shows the moisture and wind map, for the area where the ship tracks are located.

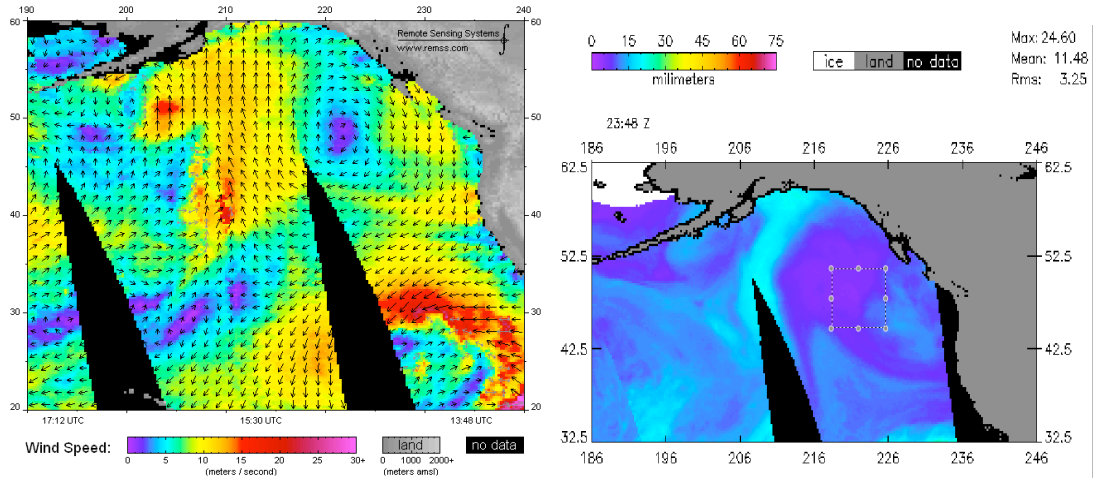

Figure 5.5 : Wind map and moisture map for North Pacific Ocean case.

For this case, the wind is northerly with speed around 10 knots and the moisture values are up to 15 millimeters and there is no significant moisture gradient for the ship track area. Figure 5.6 shows the growth of the particles in time for five different plumes for Aqua and Terra imagery and their comparisons for each plume.

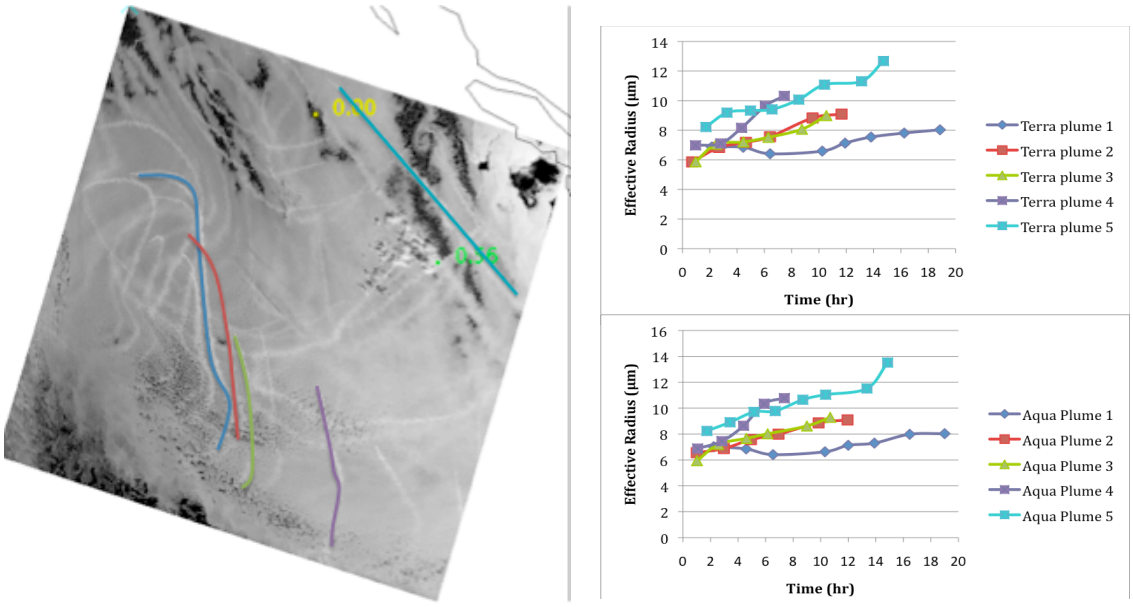

Figure 5.6 : Effective radius change with time for Terra and Aqua MODIS and their comparisons for each plume for North Pacific Ocean case.

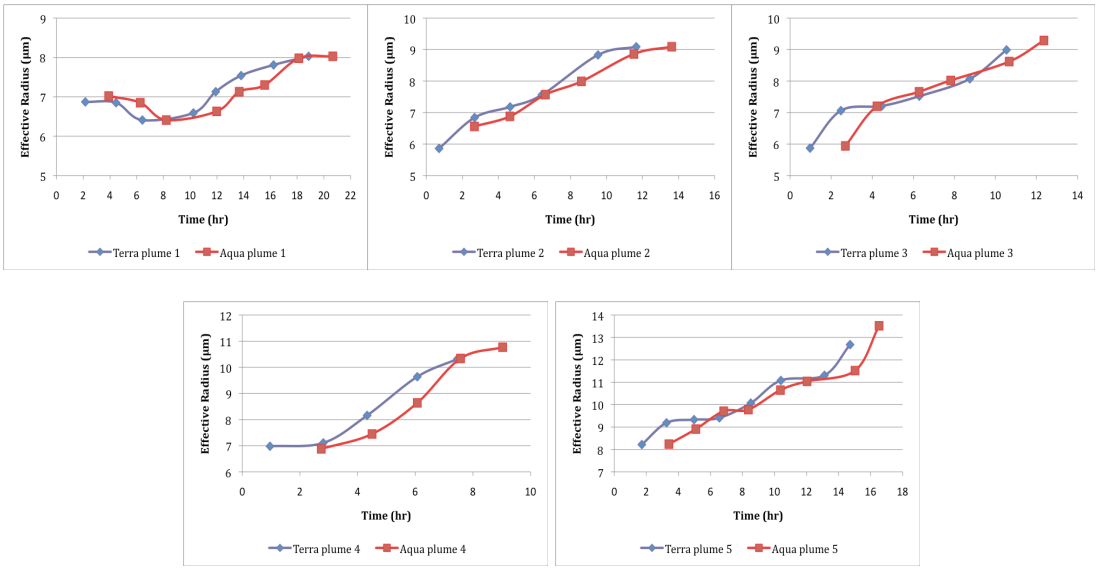

Figure 5.6 (contd.) : Effective radius change with time for Terra and Aqua MODIS and their comparisons for each plume for North Pacific Ocean case.

Blue, red, green, purple and cyan colors represent plume 1, plume 2, plume 3, plume 4 and plume 5, respectively. Terra and Aqua datasets with 1 km resolution cover the same region with 105 minutes time difference. The graphs show the particle size change over time for the selected plumes for Terra and Aqua data. The rate of change is calculated to be 0.1 to 0.5 microns per hour for Terra while it is 0.1 to 0.6 microns per hour for Aqua. Again, Aqua and Terra have almost the same trend. The correlation between two sensors is calculated to be .90 to .95.

Figure 5.7 shows the true color image for Terra satellite over the North Pacific Ocean where the ship tracks are located.

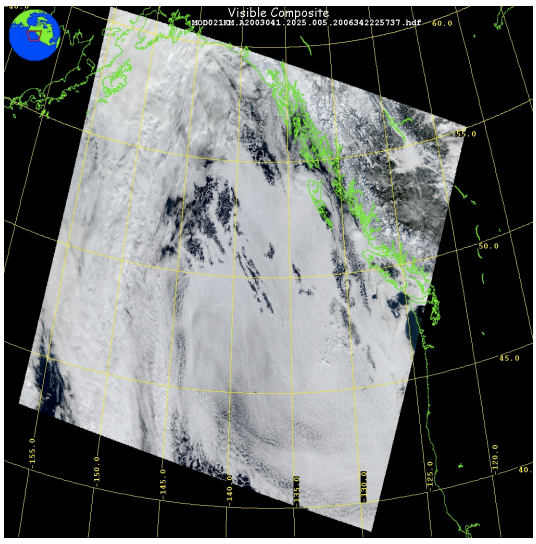

Figure 5.7 : Real time Terra image for North Pacific Ocean case.

Air over ocean is usually cleaner than air over land; over large water bodies, there are fewer particles to form cloud droplets. Due to the ship emissions, smaller and numerous particles release from ship stacks into marine atmosphere and form ship tracks with high reflectance, thus brighter than its vicinity. For this case ship tracks can still be discriminated from background clouds even though the background is almost as bright as the ship track is.

In Figure 5.7, ship tracks are hard to discriminate. This might be because the background cloud layer was already quite bright.

5.3 Alaska Case Study

On March 4, 2009, Terra and Aqua satellites observed ship tracks over the North Pacific Ocean, south of Alaska. Figure 5.8 shows the how ship tracks seem different than the natural marine clouds for the same area. They appear brighter than the natural marine cloud layer.

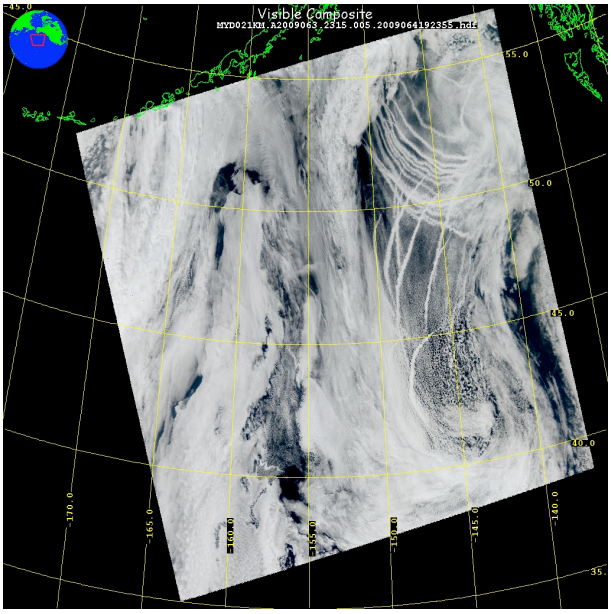

Figure 5.8 : Ship tracks south of Alaska.

Effective radius change with time with using MOD06 cloud product is given in Figure 5.9. The time difference between Terra and Aqua is 110 minutes, so basically this figure shows the particle size change in 110 minutes.

Cloud particle growth as a function of time is studied for five ship tracks in both datasets.Blue, red, green, purple and cyan colors represent plume 1, plume 2, plume

3, plume 4 and plume 5, respectively. The vertical plumes are easy to detect from start to finish and hence are studied here. The horizontal plumes lie under the marine stratus layer and that makes the starting points of the plumes hard to detect.

The growth of the particle size for each of the plumes is calculated to be 0.6 to 1.2 microns per hour for Terra and 0.8 to 1.2 microns per hour for Aqua. Terra and Aqua sensors' results were seemed to be equal. These two sensors are .86 to.98 correlated with each other.

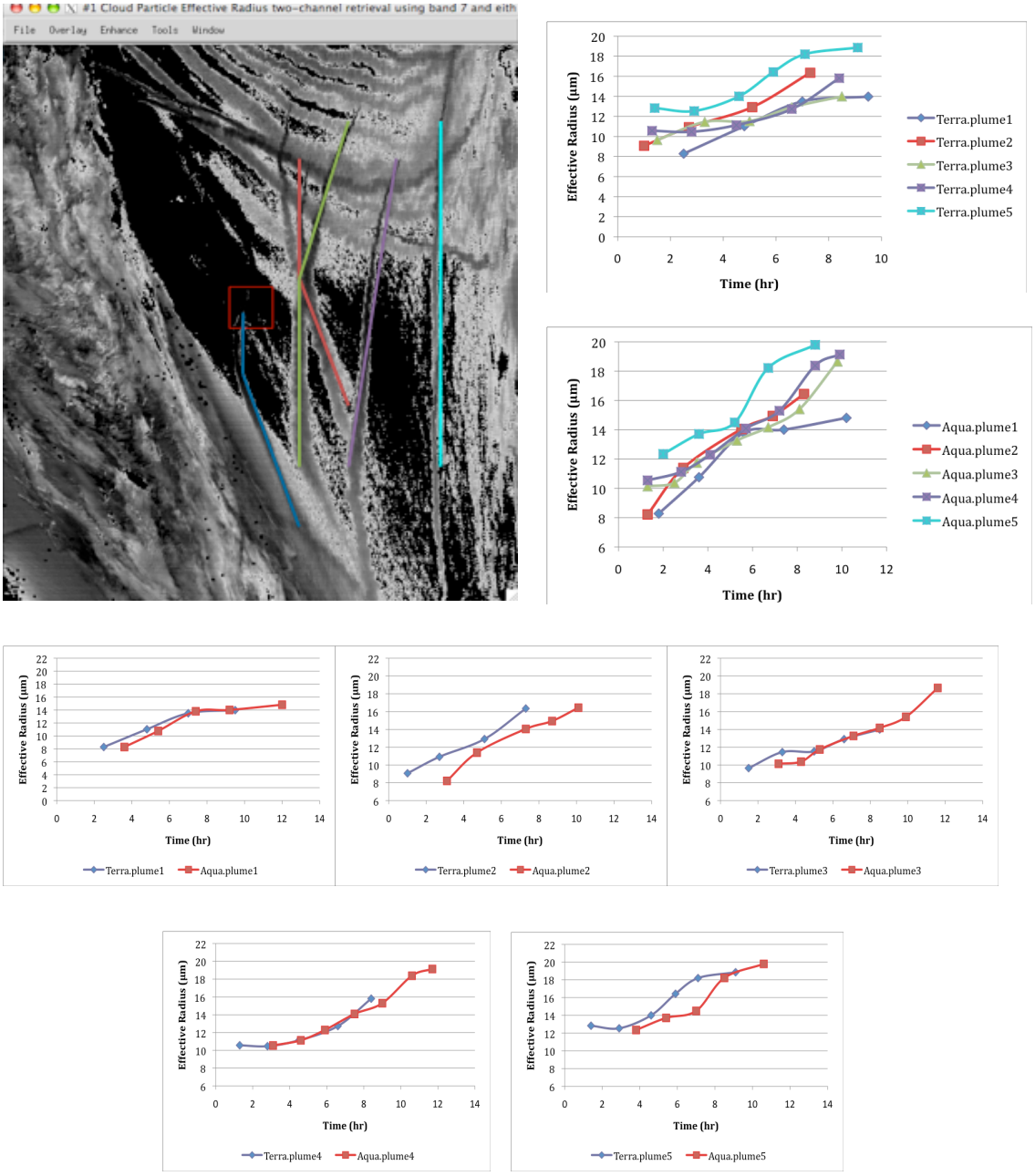

Figure 5.9 : Effective radius change with time for MODIS Aqua and MODIS Terra and their comparisons for each plume for Alaska case.

Figure 5.10 shows the atmospheric parameters, which may effect the ship track formation. Wind map is obtained from Quickscat data and moisture map is obtained from AMSR-E data.

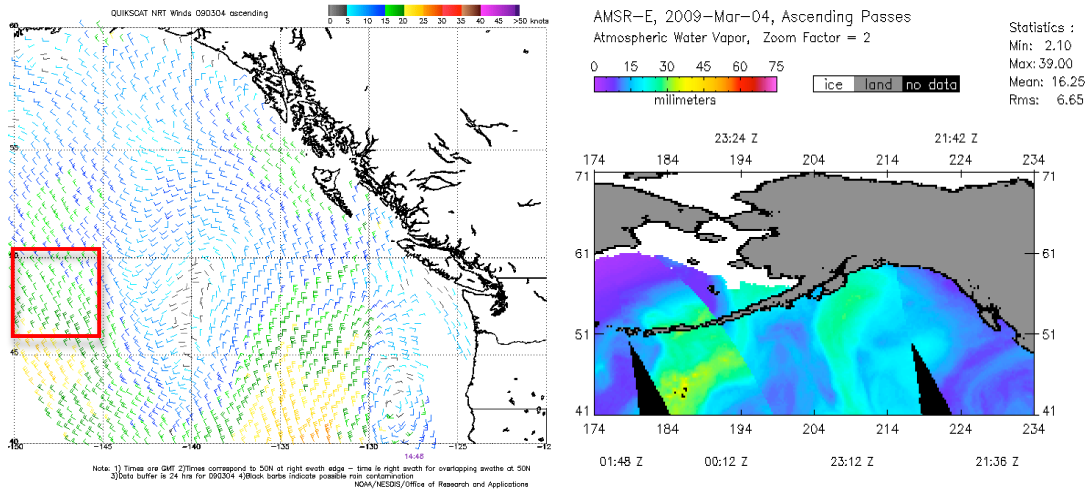

Figure 5.10 : Wind map and moisture map for Alaska case study.

The wind speed is between around 15 knots and the wind is turning anticyclonically over the region where ship tracks are located, thus they have a curved appearance. The moisture value is around 20 millimeters. There is no strong moisture gradient for the area where ship tracks are located. In track and out-of-track regions may contain the same volume of water. The particles in the tracks are smaller and numerous than the particles out-of track regions due to pollutants in the ship exhaust. According to the moisture content of the air above the clouds, the polluted clouds, such as ship tracks, could either gain or lose water content (Segrin et al., 2007). A study done at NASA Ames Research Center (2005) also indicates that when air over a cloud is humid, cloud water increases in polluted clouds. However, the water decreases in polluted clouds when air over a cloud is dry, which is consistent with the behavior of ship track observations.

5.4 Kuril Islands Case Study

The next case study is on July 2, 2003, over the Pacific Ocean off the coast of Kuril Islands. Plumes are identified in both the Terra and Aqua images by shape and location. The observations were made at 00:50 UTC by the Terra satellite and at 02:30 UTC by the Aqua satellite. During these 100 minutes, the ship track plumes grew longer due to the ship movement and local wind vector. Figure 5.11 shows the

wind map and moisture map for the area where ship tracks were formed.

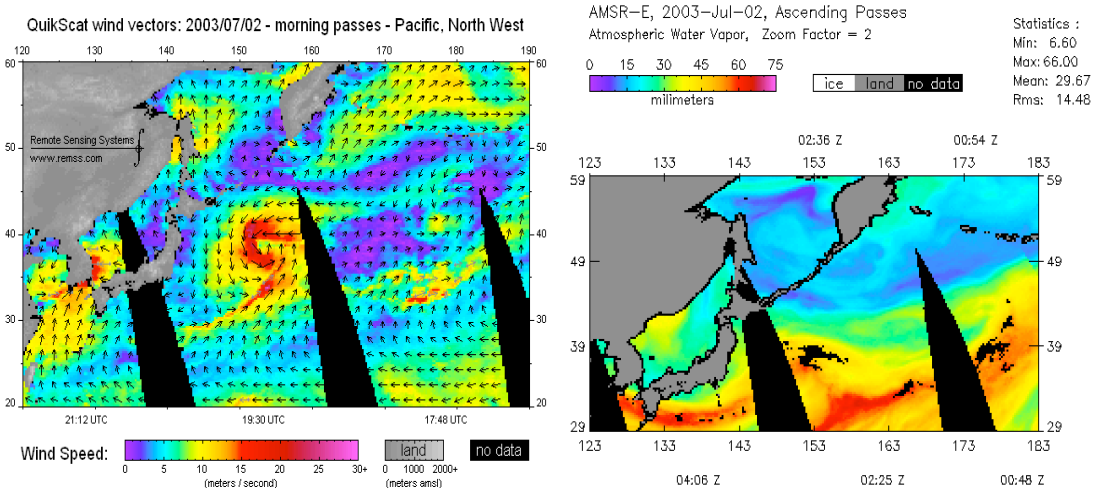

Figure 5.11 : Wind map and moisture map for Kuril Islands case.

The wind speed of the ship track region is around 7 m/s which is approximately 15 knots. The moisture map indicates values around 15 mm. One of the conditions of ship track formation is relatively small changes of humidity values. Around the Kuril Islands area the moisture gradient is small and stays at almost the minimum value through out, which is conducive to ship track formation.

Figure 5.12 shows the effective radius change with time for Terra and Aqua MODIS data.

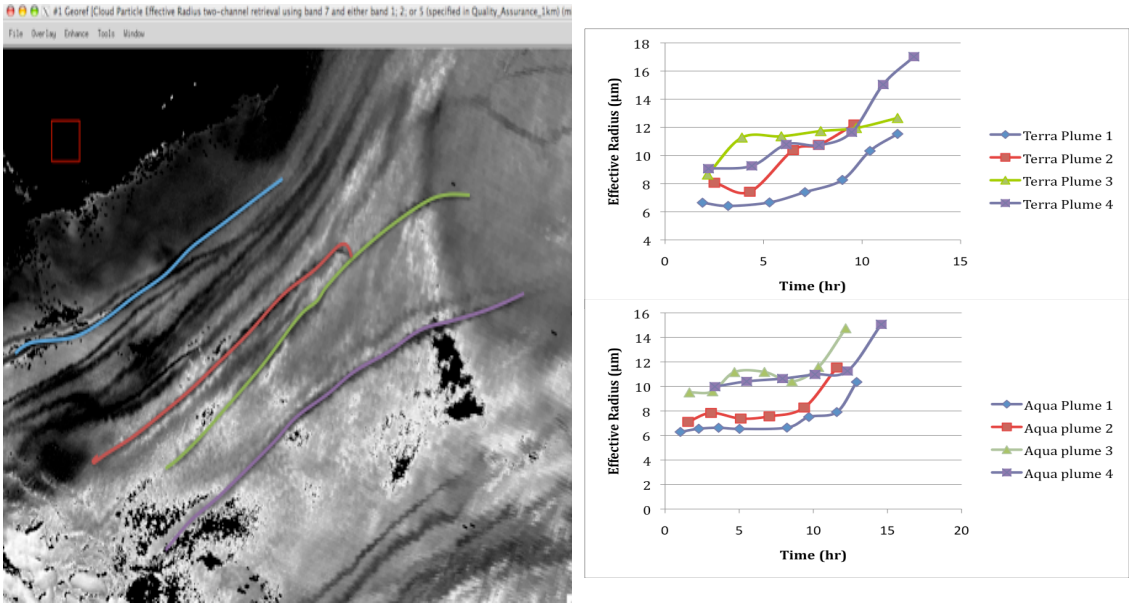

Figure 5.12: Effective radius change with time for MODIS Aqua and MODIS Terra and their comparisons for each plume for Kuril Islands case.

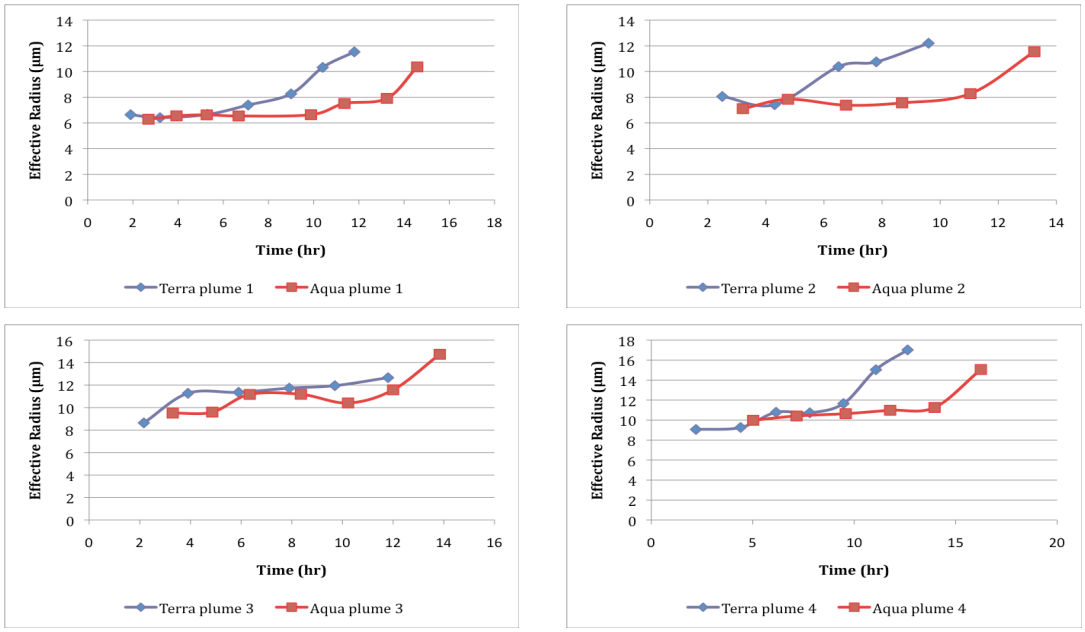

Figure 5.12 (contd.) : Effective radius change with time for MODIS Aqua and MODIS Terra and their comparisons for each plume for Kuril Islands case.

The Terra-Aqua comparison for every plume selected on the imagery is done accordingly.

Blue, red, green and purple colors represent plume 1, plume 2, plume 3 and plume 4 respectively. The growth of the particle size of each plume is calculated to be 0.4 to 0.8 µm per hour for Terra and 0.3 to 0.5 µm per hour for Aqua and the correlation between two sensors are found to be .84 to .98.

The difference between Aqua and Terra MODIS may be because of the viewing geometry and solar angle. MODIS's 110-degree field of view, sweeps out a ground swath around 2330 km wide. This swath width depends on earth curvature effects. The 55-degree scan angle, which is relative to nadir, may increases to 65-degrees due to the earth curvature (Ahmad et al., 2002). Terra is an EOS-AM satellite moving from north to south, and Aqua is EOS-PM satellite moving south to north and they sweep the same area at the same time every day. Since there is a time difference between Aqua and Terra MODIS, between two observations, sun angles also change.

Figure 5.13 shows a model of MODIS data acquisition on EOS-AM (Terra) satellite and its viewing geometry.

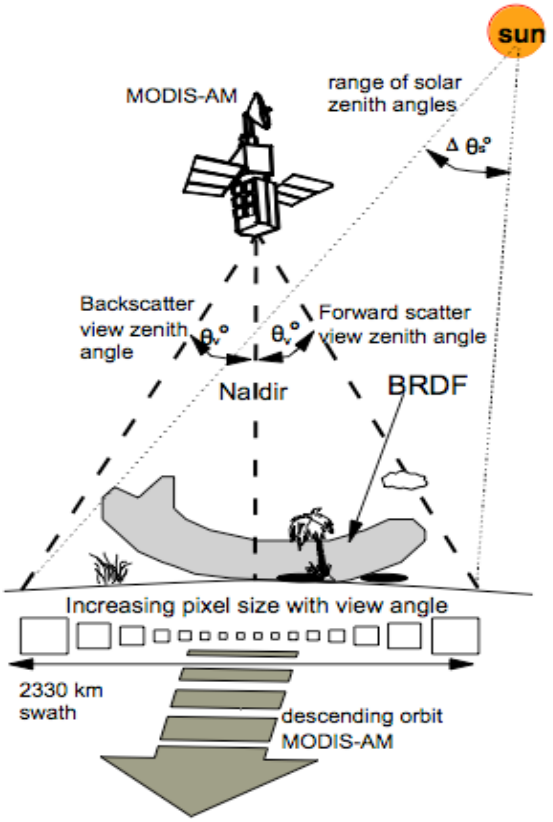

Figure 5.13 : MODIS-AM platform, data acquisition example (Huete et al.,1999).

Terra has a descending orbit (in the morning) and the sun glint region is to the east with the backscattered region to the west along its path. Conversely, Aqua has an ascending orbit and ultimately the opposite tilt. Due to the different orbits and viewing geometries, the area observed by Terra could be in the forward scattered view zenith angle direction while the same area observed later by Aqua becomes a backscattered case. Sometimes, the selected area is on the edge of the scan within the image, which is then distorted and difficult to analyze. Also, due to the time difference between two satellites, the ship tracks observed in the morning pass occasionally disappear or change form due to the dispersion by the time of afternoon pass (Christensen, 2008). Despite these difficulties, Terra and Aqua MODIS give the same trends of the particle size growth with time. The difference between the Terra and Aqua values may depend on the different viewing angle geometry.

BRDF refers to biodirectional reflection distrubution function which shows how light is reflected at an opaque surface. It changes with the view and solar angles (Huete et al.,1999).

5.5 Europe Case Study

Terra MODIS and Aqua MODIS observed ship track formation off of the coasts of France and Spain on February 25, 2005. An important difference between cloud formed from natural cloud condensation nuclei (like dust or sea salt) and ship track is, they form around the particles in ship exhaust. Thus, they are an example of anthropogenic cloud formation. The particles forming the ship track stretch over a narrow long path due to the wind direction. Figure 5.14 shows the wind and moisture maps for Europe case. AMSR-E data is used to get moisture map, for wind map Seawinds data is used.

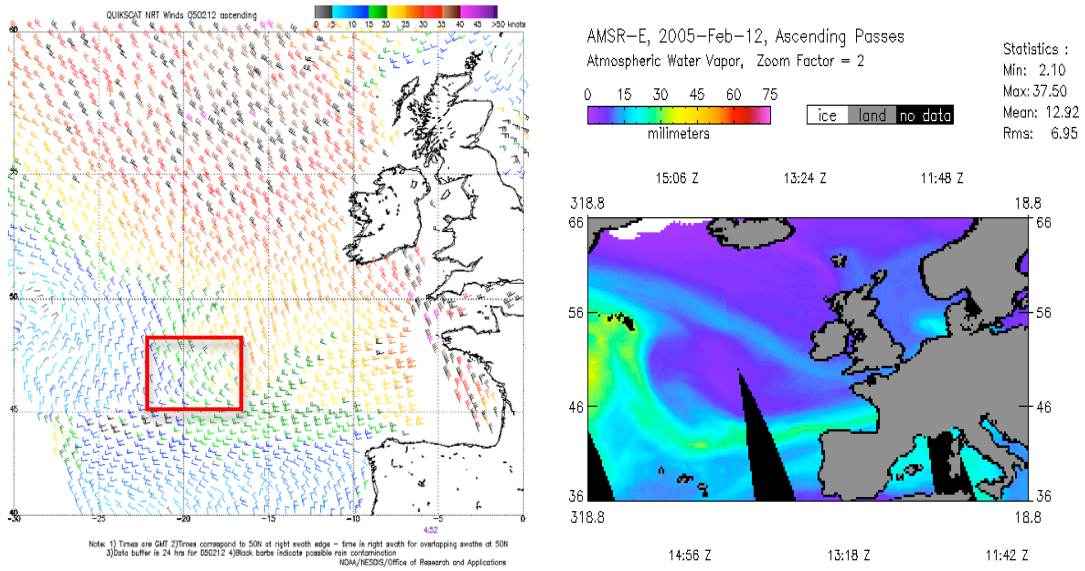

Figure 5.14: Wind and moisture map for Europe case.

Northerly winds are observed off the coast of France and Spain with speed around 15 knots and the moisture values are approximately 15 millimeters. Wind is an important meteorological parameter because the position of the ship track changes due to the direction of the wind.

Ship tracks chosen to be common in both Terra and Aqua imageries. The near infrared reflectance, which is related to MOD06 cloud product, is used to observe particle size change of ship tracks observed from Aqua and Terra satellite. Figure 5.15 shows the effective radius change over time for the four plumes on both Terra and Aqua image and their comparisons.

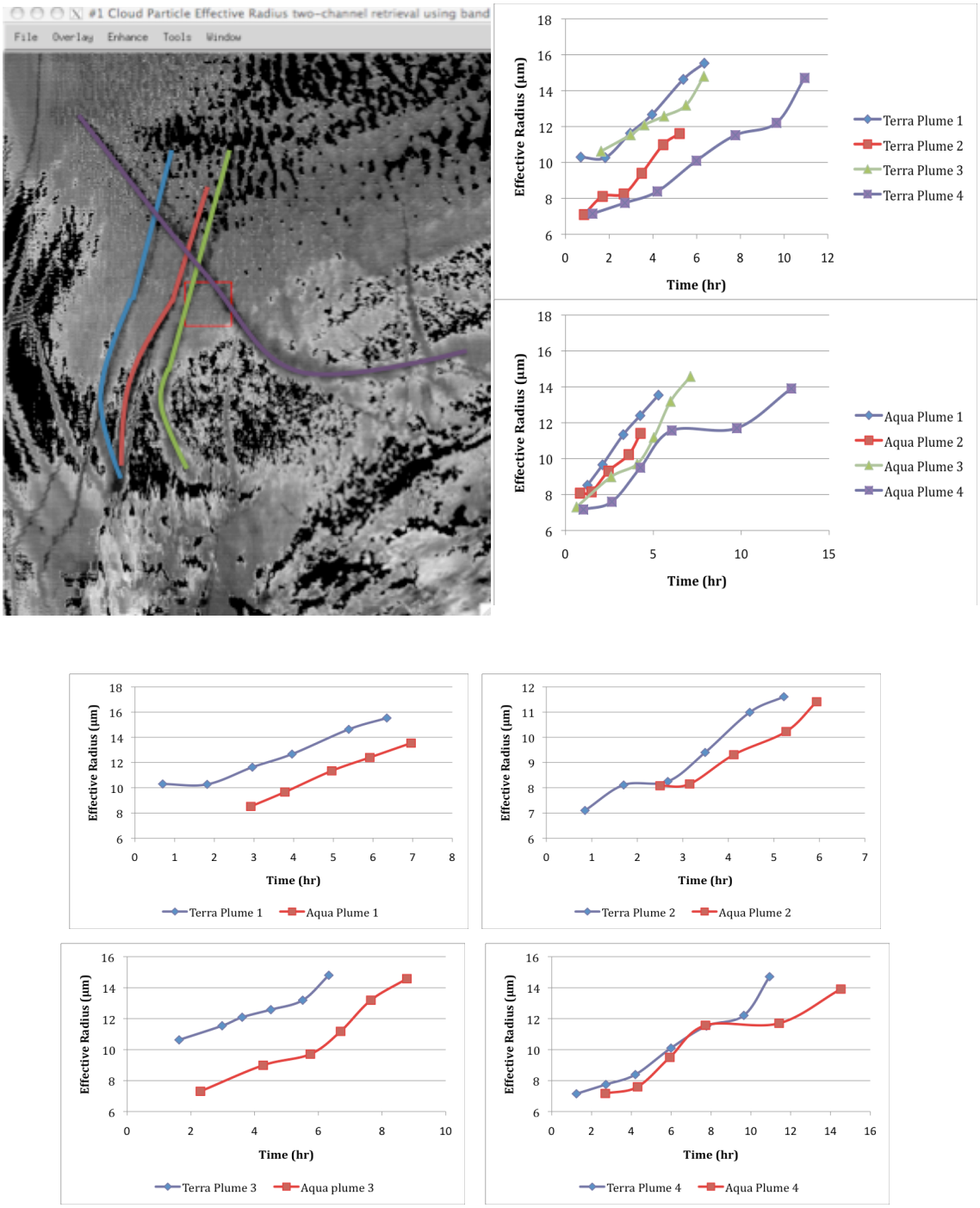

Figure 5.15 : Effective radius change with time for MODIS Aqua and MODIS Terra and their comparisons for Europe case.

Blue, red, green and purple colors represent plume 1, plume 2, plume 3 and plume 4 respectively. Those tracks are analyzed to study the growth of particles from the morning to afternoon time period. Time difference between two observations is 100 minutes. The growth of the particle size of each plume is calculated to be 0.8 to 1.0 µm per hour for Terra and 0.6 to 1.2 µm per hour for Aqua. Both Terra and Aqua have an increasing trend and the correlation between two sensors is .83 to .98.

An attempt was made to infer the particle growth with time over the same area using SEVIRI (Spinning Enhanced Visible and Infrared Imager) data. The main optical payload on board of the Second-generation Meteosat platform, SEVIRI, has twelve spectral channels (including visible and 1.6 μm), which provide accurate weather monitoring data with a repeat cycle of 15 minutes and 3 km spatial resolution (EUMETSAT, 2010). Effective radius was estimated with SEVIRI data, however the SEVIRI results (not shown) were not comparable to MODIS results because the spatial resolutions and viewing geometries are very different. However the study of ship tracks with MODIS data at 1 km resolution could be complemented with SEVIRI data observed every 15 minutes, when some of the diffences in viewing geometry, spectral coverage, and spatial resolution are resolved (this would a be a useful follow-on work to this thesis).

6. RESULTS OF CASE STUDIES

Five case studies, off the coast of California, over North Pacific Ocean, south of Alaska, off the coast of Kuril Islands, Eastern Russia and off the coast of Spain and France over Atlantic Ocean, are chosen to investigate the effective radius change with time. The 1 km MODIS measurements for the morning passes of the Terra and the afternoon passes of the Aqua satellites are analyzed along with the MOD06 cloud product. Ship tracks are chosen that are found in both Terra and Aqua images. The MOD06 cloud algorithm provides products relevant to the optical and thermo dynamical properties of cloud layers such as optical thickness, effective particle radius, and particle phase. Effective particle radius, which can also be defined as particle size, is an area weighted mean radius of the particles. The algorithm is based on the reflection function, which is related to viewing angle and solar angles. MOD06 algorithm is typically based on three different band combinations (1.64, 2.13, and 3.75 μm). 2.13 μm is a very useful band to detect ship tracks due to the reflection difference between sea surface and the ship exhaust.

A Haversine formula, which is based on great-circle distances between the two points, is used to calculate the distance between ship locations in the Terra and Aqua images. Since the time difference between two sensors is known, the speed of the vessel is estimated. Effective cloud particle radii are studied along a transect perpendicular to the ship track, away from ship track intersections.

Ouickscat data is used for wind speed estimations and AMSR-E for moisture.

Information about all case studies is summarized in Table 6.1. Common plumes are chosen in both Terra and Aqua imageries to estimate the particle size change. For the California case the particle growth with time is found to be 0.3 to 0.8 μm for Terra and 0.5 to 1.0 μm for Aqua. For the North Pacific Ocean case, it is calculated as 0.1 to 0.5 μm for Terra and 0.1 to 0.6 μm for Aqua. For the Alaska case, the growth of particle size is found 0.6 to 1.2 μm for Terra and 0.8 to 1.2 μm for Aqua. For the Kuril Islands case particle size is changed 0.4 to 0.8 μm for Terra and 0.3 to 0.5 μm

for Aqua. It is found to be 0.8 to 1.0 µm for Terra and 0.6 to 1.2 µm for Aqua for the Europe Case. The two sensor's effective radius values for each selected common plume are correlated with each other. It is calculated to be .86 to .98 for the California case, .90 to .95 for the North Pacific Ocean case, .81 to .98 for the Alaska case, .84 to .98 for the Kuril Islands case, .83 to .98 for the Europe case.

Table 6.1 : Summary of all case studies.

CASE NAME	*CALIFORNIA CASE*	*NORTH PACIFIC CASE*	*ALASKA CASE*	*KURIL ISLANDS CASE*	*EUROPE CASE*
DATE	2005, September 30	2003, February 10	2009, March 4	2003, July 2	2005, February 12
DATA	Terra MODIS Aqua MODIS	Terra MODIS Aqua MODIS	Terra MODIS Aqua MODIS	Terra MODIS Aqua MODIS	Terra MODIS Aqua MODIS
TIME between two sensors	95 minutes	105 minutes	110 minutes	100 minutes	100 minutes
RESOLUTION	1 km	1 km	1 km	1 km	1 km
WIND SPEED	15 knots	10 knots	15 knots	15 knots	15 knots
VESSEL SPEED	~21±4 knots	~31±3 knots	~20±4 knots	~22±4 knots	~23±4 knots
MOISTURE	15 mm	15 mm	20mm	15 mm	15 mm
Paricle size growth with time	0.3-0.8 µm for Terra 0.5-1.0 µm for Aqua	0.1-0.5 µm for Terra 0.1-0.6 µm for Aqua	0.6-1.2 µm for Terra 0.8-1.2 µm for Aqua	0.4-0.8 µm for Terra 0.3-0.5 µm for Aqua	0.8-1.0 µm for Terra 0.6-1.2 µm for Aqua
Correlation Between Sensors	~ .92±.06	~ .93±.02	~ .91±.07	~ .91±.07	~ .91±.06
DURATION of PLUME	5 – 9 hours (According to Aqua)	7-19 hours (According to Aqua)	8-10 hours (According to Aqua)	13-16 hours (According to Aqua)	5-16 hours (According to Aqua)
Plume Length (in pixels)					
Terra Plume 1	428	874	382	716	385
Terra Plume 2	488	570	340	548	367
Terra Plume 3	396	396	536	750	488
Terra Plume 4	477	432	511	820	575
Terra Plume 5	367	826	454		
Aqua Plume 1	500	936	441	773	350
Aqua Plume 2	538	619	384	685	377
Aqua Plume 3	430	420	573	806	405
Aqua Plume 4	527	490	601	940	660
Aqua Plume 5	486	940	500		

Fuel type of the vessel is also important due to its impact on ship track formation. Ship tracks from diesel-powered ships burning MFO are brighter (at near infrared), longer, older (longer lived), and wider than ship tracks from steam turbine ships. The duration of the each plume in each case and the length of them are shown in the table. The duration of the ship tracks are found from Aqua data. The lengths of the plumes are found with pixel values. The information about the vessels could not be obtained, however, the assumptions can be made using Table 6.1 (e.g. in the Kuril Island case study, plume lengths and duration times are long compared to those in other case studies, so all the plumes of this case likely belong to diesel powered ships burning MFO; the large particle size and long duration of the plumes in the North

Pacific case also suggest diesel power for ships associated with plume 1 and 5). Figure 6.1 shows the comparisons of particle size change with time between Terra MODIS and Aqua MODIS for each case.

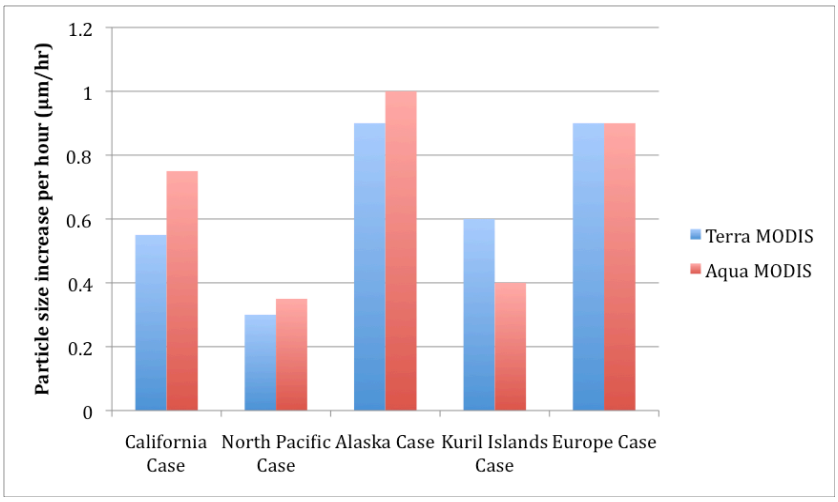

Figure 6.1 : Particle size growth with time.

It is assumed that all the plumes of the Kuril Islands case and plume 1 and 5 of North Pacific Ocean case likely belong to ships burning low grade fuel oil. Figure 6.1 shows those two case studies are associated with smaller values of particle size growth comparing to the other cases. That might be because ships burning low grade marine fuel oil emit larger particles and their growth occurs at a slower rate.

Effective particle size is found to be around 9 µm at the beginning of each ship track plume. It gets larger further down the plume away from the ship suggesting particle growth with time. Figure 6.2 shows the effective particle size of the plume at the beginning point of the ship track versus number of observations done using Terra and and Aqua MODIS.

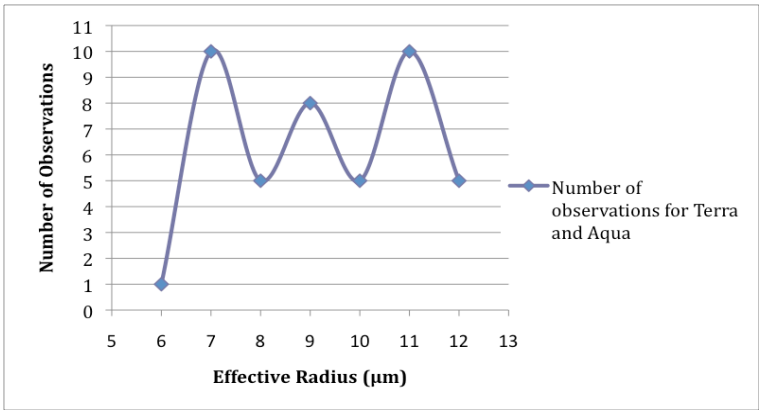

Figure 6.2 : Number of observations vs. size of the beginning values of plumes.

Particle size tends to cluster into two groups, less than and greater than 9 µm. Since larger particles indicate diesel powered ships burning MFO, then the particles greater than 9 µm can be expected to be resulting from marine fuel oil.

Same plumes over the same area are chosen in each case to run the algorithm. The difference of the values between Terra and Aqua MODIS can be due to the atmospheric parameters, the time between two sensors, or solar and sensor view angles. Terra in a descending (morning) orbit and Aqua in an ascending (afternoon) orbit have reversed viewing geometry for each case study, so Terra could be in the forward scattered view zenith angle direction while Aqua could be in a backscattered. Pixel size changes with the view angle. As the view angle approaches to nadir, the size of the pixel gets smaller, further away from nadir it gets bigger. Table 6.2 shows the view angle of the sensors for each case.

Table 6.2: View angles of the case studies.

	California Case	North Pacific Ocean Case	Alaska Case	Kuril Islands Case	Europe Case
Terra Plume 1	Beginning; near nadir End; near nadir	Beginning; near nadir End; near nadir	Beginning; near nadir End; off nadir	Beginning; off nadir End; near nadir	Beginning; off nadir End; off nadir
Terra Plume 2	Beginning; near nadir End; near nadir	Beginning; near nadir End; near nadir	Beginning; off nadir End; off nadir	Beginning; off nadir End; near nadir	Beginning; off nadir End; off nadir
Terra Plume 3	Beginning; near nadir End; near nadir	Beginning; near nadir End; off nadir	Beginning; off nadir End; off nadir	Beginning; off nadir End; off nadir	Beginning; off nadir End; off nadir
Terra Plume 4	Beginning; off nadir End; near nadir	Beginning; off nadir End; off nadir	Beginning; off nadir End; off nadir	Beginning; off nadir End; off nadir	Beginning; off nadir End; off nadir
Terra Plume 5	Beginning; near nadir End; off nadir	Beginning; near nadir End; off nadir	Beginning; off nadir End; off nadir		Beginning; off nadir End; off nadir
Aqua Plume 1	Beginning; off nadir End; off nadir	Beginning; near nadir End; near nadir	Beginning; near nadir End; near nadir	Beginning; near nadir End; near nadir	Beginning; off nadir End; off nadir
Aqua plume 2	Beginning; off nadir End; off nadir	Beginning; near nadir End; near nadir	Beginning; off nadir End; off nadir	Beginning; off nadir End; near nadir	Beginning; off nadir End; off nadir
Aqua Plume 3	Beginning; off nadir End; off nadir	Beginning; near nadir End; near nadir	Beginning; off nadir End; near nadir	Beginning; off nadir End; near nadir	Beginning; off nadir End; off nadir
Aqua Plume 4	Beginning; off nadir End; off nadir	Beginning; near nadir End; near nadir	Beginning; off nadir End; off nadir	Beginning; off nadir End; near nadir	Beginning; off nadir End; off nadir
Aqua Plume 5	Beginning; off nadir End; off nadir	Beginning; near nadir End; off nadir	Beginning; off nadir End; off nadir		Beginning; off nadir End; off nadir

Near nadir and off nadir angle information is given in the table for each plume of the case studies both for Terra and Aqua. Beginning indicates the beginning point of the plume while end indicates the end of it. Nadir points the surface directly below the sensor moving along its flight line. Near nadir represents the area close to nadir and off nadir represents the area away from the nadir. The viewing zenith angle is chosen

to be 30° on both sides of nadir. The angle greater than 30° is chosen as off-nadir angle, angle smaller than 30° is, however, chosen as near nadir angle. Off-nadir viewing angle, which usually occurs at the edge of the imagery, have more distortions with larger pixel sizes and less detail, and the features on the imagery are usually difficult to analyze. The results, however, show that two sensors estimates of effective radius have the same increasing trend and they are correlated with each other.

7. CONCLUSION

The purpose of this study was to investigate the microphysical properties of ship tracks, which are low level, anthropogenic clouds forming around the exhaust released by ships. Terra MODIS and Aqua MODIS observations of ship tracks were analyzed for five different case studies. The ship tracks in these case studies were located off the coast of California, over North Pacific Ocean, south of Alaska, off the coast of Kuril Islands and over Atlantic Ocean off the coast of Spain and France. MODIS cloud product (MOD06) data were used to estimate particle size change as a function of time. MOD06 combines infrared and visible techniques to determine both physical and radiative cloud properties, which are cloud-particle phase, effective cloud particle radius, and cloud optical thickness properties. The effective cloud particle radius product for both Aqua and Terra satellites was the best tool to guide the development and validation of this project. Terra is in descending (morning) orbit and Aqua is in ascending (afternoon) orbit and these two sensors capture the image of the same location within hours of each other. Common ship tracks in each imagery were chosen to find the particle size growth with time. The results of two sensors were correlated to each other to see whether they are in good agreement or not.

Air over the ocean is cleaner than the air over the land. Thus, there are fewer particles to act as cloud condensation nuclei. Since there are more small particles in the ship exhaust than the clean ocean air, moisture accumulates on the ship exhaust particles until a visible plume (cloud) is formed. Ship tracks enhance the reflectivity of the low level marine stratiform cloud by increasing the number of the particles and decreasing the particle size. Due to the high reflectance caused by small particles, ship tracks seem brighter than nearby areas in the imagery. The reflectance increases at longer wavelengths and thus the ship tracks are more evident in near infrared bands, 2.13 and 3.7 μm, than in visible bands, 0.8 or 0.6 μm. Research results showed that the contrast between ship tracks and nearby areas increases as the wavelength gets longer, thus they can better be detected at longer wavelengths in the

near infrared part of the spectrum.

Ship tracks basically form in the low stratiform clouds off the western coasts of large continents, where upwelling ocean currents cause a stable atmospheric layer enhancing the likelihood of the presence of saturated marine boundary layers. This creates an ideal environment for the formation of marine stratiform clouds. Ship tracks are the result of a ship passing under the stratiform cloud. When the particles enter a stratiform cloud layer in the boundary layer, they either modify the existing cloud or they act as a CCN and form cloud droplets. Not every ship produces a ship track. Ambient conditions, which are necessary before ship track formation are low level stable layer, small number concentration of CCN, and small changes at relative humidity. According to the moisture maps of the case studies, there is no moisture gradient at the areas where ship tracks are located, and the values are to be around 15 mm.

In addition to ambient marine atmospheric conditions, ship track formation depends on the fuel burned and the associated particle emission. Information about the ship and their properties could not be obtained, however some it can be inferred from the following: ship tracks from diesel ships are longer, older, and wider than ship tracks from steam turbine ships. Diesel-powered engines using MFO emit greater numbers of particles with larger radius to serve as CCN than turbine-powered engines using navy distillate fuel. So, for the same ambient condition, ship burning MFO are more likely to form a ship tracks than the ship burning high grade distillate fuel. According to the observations in this work, the particle sizes clustered into two groups, greater or smaller than 9 μm. Steam or gas turbine powered ships burning navy distillate fuel and diesel powered ships burning MFO can possibly inferred from effective partice size and length of the plume; larger particle sizes and longer plumes are expected when the oil is MFO.

Cloud particle growth in time has been studied in plumes extending up to 16 hours in the cases studied. Terra and Aqua MODIS instruments were in good agreement in their estimates of effective cloud radius, coming from the MOD06 cloud product. In addition Terra and Aqua also agreed on the change over time in the effective particle radius. The particle size was larger further down the plume away from the ship, suggesting particle growth with time in the atmosphere. The growth rate was found to be up to one micron per hour. Terra and Aqua MODIS sensors offered an

opportunity to investigate the same area within hours. The same ship track plumes were chosen to investigate the microphysical change of the cloud both in Terra and Aqua images; the correlation between the two sensors was found to be 90±8%.

This is the first study to estimate microphysical properties of ship tracks with MODIS data, in Turkey. This study, however, could not be adapted to seas of Turkey because ship tracks tend to form over open seas at the west part of large continents. Even when they formed over the seas of Turkey, no MODIS images were found over that area.

The results presented here show that, the anthropogenic emissions of ocean-going vessels modify the cloud overlying by introducing CCNs and changing the reflectance of the cloud. Due to the importance of these man-made, low-level clouds on climatology, future investigations are needed to understand the human effect on environment.

REFERENCES

Ackerman, A. S., et al., 2000: Effects of Aerosols on Cloud Albedo: Evaluation of Twomey's Parameterization of Cloud Susceptibility Using Measurements of Ship Tracks, *Journal of the Atmospheric Sciences.* Vol. 57, no. 16, pp. 2684-2695.

Albrecht, B. A., 1989: Aerosols, Cloud Microphysics and Fractional Cloudiness, *Science*. Vol. 245, no. 4923, pp. 1227-1230.

Arakawa, H., 2007. Investigation of Ship Tracks in ATSR-2 Satellite Imagery, Atmospheric, Oceanic and Planetary Physics, University of Oxford.

Arking, A., 1991: Radiative Effects of Clouds and Their Impact on Climate, *Bulletin American Meteorological Society.* Vol. 71, no 6, pp. 795-813.

Christensen, M. W., 2008. Effects of Solar Heating on the Indirect Effect of Aerosols as Deduced from Observations of Ship Tracks. *M.Sc Thesis.* Oregon State University, OR.

Chuang, C. C. and J. E. Penner, 1995: Effects of anthropogenic sulfate on cloud drop nucleation and optical properties, *Tellus*, Vol. 47B, pp. 566-577.

Coakley, J. A. Jr., et al., 1987. Effect of Ship-Stack Effluents on Cloud Reflectivity, *Science.* Vol. 237, no. 4818, pp. 1020-1022.

Coakley, J., et al., 2000. The Appearance and Disappearance of Ship Tracks on Large Spatial Scales, *Journal of the Atmospheric Sciences*, Vol. 57, pp. 2765-2778.

Conover, J. H., 1966. Anomalous Cloud Lines, *Journal of the Atmospheric Sciences,* Vol. 23, pp. 778-785.

Durkee P. A., et al., 2000a. The Monterey Area Ship Track Experiment, *Journal of the Atmospheric Sciences,* Vol. 57, pp. 2523-2541.

Durkee P. A., et al., 2000b. Composite Ship Track Characteristics, *Journal of the Atmospheric Sciences,* Vol. 57, pp. 2542-2553.

EUTMETSAT, 2010. Meteosat Second Generation Instruments. From http://www.eumetsat.int/Home/Main/Satellites/MeteosatSecondGeneration/Instruments/index.htm?l=en, accessed at 20.11.2010.

Evans, M. E., 1992. Analysis of Ship Tracks in Cloudiness Transition Regions, *M.Sc Thesis.* Naval Postgraduate School, CA.

Ferek R. J., et al., 2000. Drizzle Suppression in Ship Tracks, *Journal of the Atmospheric Sciences,* Vol. 57, pp. 2707-2728.

Huete, A., et al., 1999. MODIS Vegetation Index (MOD 13), *Algorithm Theoretical Basis Document,* Version 3.

Hobbs P. V., et al., 2000. Emissions from Ships with respect to Their Effects on Clouds, *Journal of the Atmospheric Sciences,* Vol. 57, pp. 2570-2590.

Hudson J. G., et al., 2000. Cloud Condensation Nuclei and Ship Tracks, *Journal of the Atmospheric Sciences,* Vol. 57, pp. 2696-2706.

King M. D. et al., 1992. Remote Sensing of Cloud, Aerosol, and Water Vapor Properties from the Moderate Resolution Imaging Spectrometer (MODIS), *IEEE Transactions on Geoscience and Remote Sensing,* Vol. 30, pp. 2-27.

King M. D. et al., 1997. Cloud Retrieval Algorithms for MODIS: Optical Thickness, Effective Particle Radius, and Thermodynamic Phase, MOD06 – Cloud product*, MODIS Algorithm Theoretical Basis Document,* No. ATBD-MOD-05*,* Version 5.

Movable Type Scripts, 2010. Calculate distance, bearing and more between Latitude/Longitude points, from *http://www.movable-type.co.uk/scripts/latlong.html*, accessed at 29.09.2009.

Nakajima T., King M. D., 1990. Determination of the Optical Thickness and Effective Particle Radius of Clouds from Reflected Solar Radiation Measurements. Part I: Theory, *Journal of Atmospheric Sciences,* Vol. 47, no. 15, pp. 1878-1893.

NASA/Ames Research Center, 2005. NASA Finds Polluted Clouds Hold Less Moisture And Cool Earth Less. *ScienceDaily*. from http://www.sciencedaily.com/releases/2005/01/050104072650.htm, accessed at 01.12.2010.

NASA Earth Observatory, 2008. Cloud Streets Across Caspian Sea. *Image of the Day.* From http://earthobservatory.nasa.gov/IOTD/view.php?id=8399, accessed at 14.12.2010.

NASA/Goddard Research Center, 2009. From http://disc.sci.gsfc.nasa.gov/data-holdings/PIP/, accessed at 11.11.2010.

NASA/Marshall Research Center. From http://www.ghcc.msfc.nasa.gov/AMSR/, accessed at 15.11.2010.

Öström E., et al., 2000. Cloud Droplet Residual Particle Microphysics in Marine Stratocumulus Clouds Observed during the Monterey Area Ship Track Experiment, *Journal of Atmospheric Sciences,* Vol. 57, pp. 2671-2683.

Platnick S., and Twomey S., 1994. Determining the Susceptibility of Cloud Albedo to Changes in Droplet Concentration with the Advanced Very High Resolution Radiometer, *Journal of Applied Meteorology,* Vol. 33, pp. 334-347.

Platnick S., et al., 2000. The Role of Background Cloud Microphysics in the Radiative Formation of Ship Tracks, *Journal of Atmospheric Sciences,* Vol. 57, pp. 2607-2624.

Radke L. F., et al., 1989. Direct and Remote Sensing Observations of the Effects of Ships on Clouds, *Science,* Vol. 246, pp. 1146-1149.

Remote Sensing Systems, 2009. Description of Scatterometer Data Products. From http://www.ssmi.com/qscat/qscat_description.html, accessed at 15.11.2010.

Rosenfeld D., Woodley W., 2001. Pollution and Clouds, *Physics World,* pp. 33-37.

Schreier M., et al., 2006. Impact of ship emissions on the microphysical, optical and radiative properties of marine stratus: a case study, *Atmospheric Chemistry and Physics,* Vol. 6, pp. 4925–4942.

Schreier M., et al., 2007. Global ship track distribution and radiative forcing from 1 year of AATSR data. *Geophysical Research Letters,* Vol. 34, L17814, doi:10.1029/2007GL030664.

Segrin M. S., et al., 2007. MODIS Observations of Ship Tracks in Summertime Stratus off the West Coast of the United States, *Journal of Atmospheric Sciences,* Vol. 64, pp. 4330-4345.

Straka III W., and Heidinger A. K., 2006. Comparison of the Advanced Very High Resolution Radiometer (AVHRR) and Moderate Resolution Imaging Spectroradiometer (MODIS) cloud properties using PATMOS-x, *14th Conference on Satellite Meteorology and Oceanography,* Atlanta, GE, USA, January 28-February 2.

CURRICULUM VITAE

Candidate's full name: Burcu Kabataş

Place and date of birth: Istanbul/1984

Universities and
Colleges attended: B.Sc. degree in Meteorological Engineering from Istanbul Technical University in 2008.